



Published in final edited form as:

J Med Chem. 2016 July 28; 59(14): 6753–6771. doi:10.1021/acs.jmedchem.6b00397.

Chromenopyrazole, a Versatile Cannabinoid Scaffold with in Vivo Activity in a Model of Multiple Sclerosis

Paula Morales[†], María Gómez-Cañas^{#,†,§}, Gemma Navarro^{#||}, Dow P. Hurst^{‡,⊥}, Francisco J. Carrillo-Salinas[#], Laura Lagartera[†], Ruth Pazos^{‡,§}, Pilar Goya[†], Patricia H. Reggio[⊥], Carmen Guaza[#], Rafael Franco^{||}, Javier Fernández-Ruiz^{‡,§}, and Nadine Jagerovic^{*,†}

[†]Instituto de Química Médica, Consejo Superior de Investigaciones Científicas, Calle Juan de la Cierva, 3, E-28006 Madrid, Spain

[‡]Instituto Universitario de Investigación en Neuroquímica, Departamento de Bioquímica y Biología Molecular, Facultad de Medicina, Universidad Complutense de Madrid, E-28040 Madrid, Spain

[§]Centro de Investigación Biomédica en Red sobre Enfermedades Neurodegenerativas (CIBERNED), and Instituto Ramón y Cajal de Investigación Sanitaria (IRYCIS), E-28040 Madrid, Spain

^{||}Departamento de Bioquímica y Biología Molecular, Facultad de Biología, Universidad de Barcelona, E-08028 Barcelona, Spain

[⊥]Department of Chemistry and Biochemistry, University of North Carolina Greensboro, Greensboro, North Carolina 27402, United States

[#]Grupo de Neuroinmunología Neurobiología Funcional y de Sistemas, Instituto Cajal, Consejo Superior de Investigaciones Científicas, E-28002 Madrid, Spain

[#] These authors contributed equally to this work.

Abstract

*Corresponding Author Phone: +34-91-562-2900. Fax: +34-564-4853. nadine@iqm.csic.es.

Notes

The authors declare no competing financial interest.

Supporting Information

The Supporting Information is available free of charge on the ACS Publications website at DOI: 10.1021/acs.jmed-chem.6b00397. cAMP accumulation assay in nontransfected HEK293 cells; conformational analysis of **5**, **42**, **7b**, **18** and **14** and electrostatic potential map of **14**; **5**, **7**, and **18**/CB₁R* docking studies; pairwise interaction energies for **5**, **7b**, and **42** at CB₁R* and for **42** and **18** at CB₂R* model; comparison of molecular electrostatic potential maps for highly selective CB₁R (**5**) vs CB₂R (**43**) ligands; in silico ADME descriptors; and binding to plasma proteins: SPR-biosensor analysis (PDF)

SMILES data (XLS)

Docking compound **5** in CB₁ active state (PDB)

Docking compound **5** in CB₂ active state (PDB)

Docking compound **7b** in CB₁ active state (PDB)

Docking compound **7b** in CB₂ active state (PDB)

Docking compound **18** in CB₁ active state (PDB)

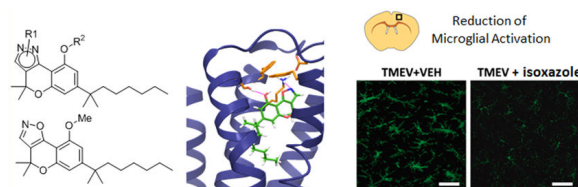
Docking compound **18** in CB₂ active state (PDB)

Docking compound **42** in CB₁ active state (PDB)

Docking compound **42** in CB₂ active state (PDB)

A combination of molecular modeling and structure–activity relationship studies has been used to fine-tune CB₂ selectivity in the chromenopyrazole ring, a versatile CB₁/CB₂ cannabinoid scaffold. Thus, a series of 36 new derivatives covering a wide range of structural diversity has been synthesized, and docking studies have been performed for some of them. Biological evaluation of the new compounds includes, among others, cannabinoid binding assays, functional studies, and surface plasmon resonance measurements. The most promising compound [**43** (PM226)], a selective and potent CB₂ agonist isoxazole derivative, was tested in the acute phase of Theiler's murine encephalomyelitis virus-induced demyelinating disease (TMEV-IDD), a well-established animal model of primary progressive multiple sclerosis. Compound **43** dampened neuroinflammation by reducing microglial activation in the TMEV.

Graphical abstract



INTRODUCTION

The endocannabinoid system (ECS) composed of at least two cannabinoid G-protein coupled receptors (CB₁ and CB₂ receptors),^{1,2} endogenous ligands such as anandamide and 2-arachidonoylglycerol, and the enzymes for their biosynthesis and degradation, is involved in numerous physiological and pathological conditions.^{3–6} Therefore, for several years the ECS has been considered a potential therapeutic target for the clinical management of various disorders including inflammatory and neuropathic pain, neurological pathologies, and cancer among others.⁷ A few diseases can be treated nowadays with cannabinoid-based medicines, mainly, plant derived compounds. A mixture of synthetic tetrahydrocannabinol (⁹-THC) [Figure 1] and nabilone, a ⁹-THC synthetic analogue, can be prescribed in several countries as antiemetic drugs for chemotherapy-induced nausea and vomiting^{8,9} and for anorexia¹⁰ treatment in patients with AIDS. A combination of ⁹-THC and cannabidiol is used for the symptomatic relief of spasticity in adults suffering multiple sclerosis and as an adjunctive analgesic treatment in adult patients with neuropathic pain or cancer.¹¹ Rimonabant, a CB₁ receptor antagonist/inverse agonist, commercialized in 2006 for the management of obesity,¹² was withdrawn a few years later because of the increase of depression, anxiety, headache, and suicidal thoughts. Even though the CB₁/CB₂ receptor agonists are currently in the forefront of clinical research for different applications, there is an increasing interest in exploiting novel pharmacological strategies.¹³ Whereas the CB₁ receptor is abundantly expressed in the central nervous system, the CB₂ receptor is mainly associated with the peripheral immune system. The CB₂ receptors are also expressed in the central nervous system in microglia and neuronal cells.^{14–18} Therefore, CB₂ receptor selective agonists exhibit a promising therapeutic potential for treating various pathologies while avoiding the adverse psychotropic effects related to the modulation of the CB₁ receptors in the brain.¹⁹ Different therapeutic applications have been proposed for CB₂

receptor agonists. Treatment of neuropathic²⁰ and osteoarthritis pain,²¹ and diagnosis and treatment of osteoporosis²² are currently in advanced development.²³ Activation of CB₂ receptors offers an attractive opportunity for treating neuroinflammatory events in neurological disorders, such as multiple sclerosis, cerebral ischemia, and Alzheimer's and Parkinson's diseases.^{13,24–31} Cannabinoid-based therapies are already approved for multiple sclerosis-associated symptoms such as pain and spasticity. The development of CB₂ receptor ligands to regulate neural inflammation and neurogenesis in multiple sclerosis is much more recent.^{30,32}

Different structures endowed with CB₂ receptor affinity and partial or full selectivity were identified mainly by pharmaceutical companies through high throughput screening as reviewed recently by Han et al.³³ In an attempt to target the CB₂ type receptor, we decided to conduct structure–activity relationship studies around the chromenopyrazole scaffold. In previous studies, we had identified chromenopyrazoles as a novel cannabinoid scaffold which leads to nonpsychoactive and selective CB₁ agonists with peripheral antinociceptive properties (Figure 1).³⁴ On the basis of these previous findings, structural modifications around the chromenopyrazole have been explored to achieve CB₂ receptor selectivity. From combined pharmacological and modeling studies, 36 new compounds covering structural diversity have been synthesized and evaluated. Among them, the most promising, **43**, a fully selective CB₂ agonist, has shown activity in the acute inflammatory phase of TMEV-IDD, a well-established animal model of primary progressive multiple sclerosis.³⁵

Synthesis

Compounds **5–39** were synthesized as depicted in Scheme 1 from 7-(1,1-dimethylheptyl)-5-hydroxy-3-(hydroxymethylen)-2,2-dimethylchroman-4-one (**4**). At the outset, chromanone **4** was prepared by demethylation of the commercially available 5-(1,1-dimethylheptyl)-1,3-dimethoxybenzene (**1**) followed by treatment with 3,3-dimethylacrylic acid and α -formylation.³⁴

Then, condensation of the β -ketoaldehyde **4** with the appropriate hydrazine gave the corresponding chromeno[4,3-*c*]pyrazol-9-oles **5–14** following a procedure previously published by us for **5–9**.³⁴ Two regioisomers, N1- and N2-substituted pyrazoles, can be formed and their structures could be observed thanks to the combined ¹H, ¹³C, HSQC, and HMBC-NMR spectra. From alkylhydrazines, the regioisomers **7a/7b** and **10a/10b** were isolated with relative ratios varying from 1/5 to 2/1 (N1/N2). Condensation with hydroxymethylhydrazine only generated N2-pyrazole substitution (**11**) probably due to steric and electrostatic repulsions. In the case of arylhydrazines and cyclohexylhydrazine, the N1-regioisomers (**8**, **9**, **12**, and **13**) were formed.

Preparation of compounds **15–39** was achieved by phenolic alkylation of the appropriate chromenopyrazoles (**5–9**) with the corresponding alkyl halide.

To explore the structure–activity relationships (SAR) on phenol substitution, conformationally restricted analogues (**40** and **41**) adopting a semiplanar geometry were synthesized as described in Scheme 2. Cyclodehydration of chromenopyrazoles **30** and **31** with phosphorus pentoxide provided the desired condensed cyclic ethers **40** and **41**.

Further exploration of chromenopyrazoles as a scaffold led us to consider the bioisosteric replacement of the pyrazole into an isoxazole moiety. For that purpose, condensation of β -diketone **4** with isoxazole **42** was efficiently achieved upon reaction with hydroxylamine hydrochloride as shown in Scheme 3. Phenolic alkylation of the chromenoisoxazole **42** yielded the methoxy (**43**) and the hydroxypropoxy (**44**) chromenoisoxazole derivatives (Scheme 3).

RESULTS AND DISCUSSION

Receptor Affinity

Chromenopyrazoles and chromenoisoxazoles **5–44** were evaluated for their ability to compete with the binding of the radiolabeled nonselective agonist [^3H]-CP55,940 to human CB₁ (hCB₁) and CB₂ (hCB₂) cannabinoid receptors. As a source for these receptors, commercial membrane preparations of HEK293 cells stably expressing the respective receptor type were used. Tables 1–3 list the affinity constant values (K_i) for hCB₁ and hCB₂ receptors obtained by fitting data from competition curves.

In prior studies, we have reported fully selective CB₁ agonists **5–6** and **9**.³⁴ On the basis of these previous findings, we have explored the SAR around the chromenopyrazole scaffold in order to achieve affinity and selectivity for the other cannabinoid receptor type CB₂. In the course of these studies, molecular modeling (discussed below) helped us to identify the structural features necessary to fine-tune CB₂ affinity and selectivity. The best results in terms of CB₂ affinity were obtained for the chromenopyrazole **34** and the chromenoisoxazole **42** with $K_i < 6$ nM. In what concerns CB₂ receptor affinity and selectivity, the chromenoisoxazole **43** (PM226)³⁶ showed CB₂ selectivity with a K_i value of 12.8 ± 2.4 nM.

In order to highlight SAR, the results may be discussed taking into account structural modifications on the pyrazole substituent (Table 1), on the phenol substituent (Table 2), and on the chromenopyrazole scaffold (Table 3).

The nature of the pyrazole substituent clearly influenced the affinity for cannabinoid receptors (Table 1). *N*-Methyl, *N*-ethyl, or unsubstituted chromenopyrazoles (**5–7**) bearing a free phenol group showed significant to high CB₁ affinity and selectivity independently of the substitution position on the pyrazole ring (N1 or N2).³⁴ *N*-Cyclohexyl substitution (**14**) drastically changed the selectivity profile exhibiting preference for the CB₂ receptor. The role played by the cyclohexyl moiety for binding to the CB₂ receptor is discussed later in the Molecular Modeling section. The presence of *N*-hydroxyalkyl groups (**10a**, **10b**, and **11**) resulted in moderate to high affinities for both receptors. Aromatic *N*-substituents (**8**, **9**, **12**, and **13**) did not turn out to be beneficial for CB₂ affinity.

Regarding the O-alkylated chromenopyrazoles (Table 2), in general, the loss of the free phenolic group led to compounds displaying high to moderate CB₂ affinity and selectivity. Modeling studies on the hydroxychromenopyrazole **7b** and methoxychromenopyrazole **18** allowed us to determine critical interactions in the CB₁ and CB₂ receptor binding sites (discussed below).

It is interesting to note that the condensation of a 2,4-dihydropyran to the chromenopyrazoles structure (**40** and **41**), which was performed for restricted conformational issues, elicited excellent CB₂ selectivity even though they showed moderate affinity. In the O-alkylated series (Table 2), the pyrazole substitution contributes to determine affinity and selectivity issues. Unsubstituted pyrazoles **15**, **22**, **28**, and **34** revealed high affinity toward both receptors regardless of the nature of the phenol substitution. *N*-Aryl substitution (**19**, **20**, **26**, **27**, **32**, and **33**) led to inactive derivatives, while *N*-methyl or ethyl substituents (**16**, **18**, **23**, **25**, **28**, **31**, **35**, and **39**) resulted in high to moderate CB₂ affinity and selectivity independently of the nature of the phenol substituent. These results suggest that the CB₂ receptor binding site does not tolerate bulky aromatic substituents on the pyrazole ring.

Bioisosteric replacement of the pyrazole by an isoxazole (Table 3) led to very potent cannabinoid ligands. Chromenoisoxazole **42** exhibited high affinity for both CB₁ and CB₂ receptors with K_i values in the low nanomolar range (K_i CB₁ = 15.4 nM; K_i CB₂ = 5.3 nM). The fact that this isoxazole derivative (**42**) but not its pyrazole analogue (**5**) binds to the CB₂ receptor has been instrumental to propose a docking mode of these compounds to the active CB₂ receptor model (CB₂R*) as discussed in the Molecular Modeling section. Furthermore, these results and the data obtained for O-alkylated chromenopyrazoles prompted us to synthesize the methoxychromenoisoxazole **43**, which resulted in the most potent and CB₂ selective ligand in this study, which was over 3000-fold selective for the CB₂ receptor with an affinity constant of 12.8 nM. This CB₂ affinity was similar to that of other selective synthetic CB₂ receptor agonists, [(1*R*,2*R*,5*R*)-2-[2,6-dimethoxy-4-(2-methyloctan-2-yl)phenyl]-7,7-dimethyl-4-bicyclo-[3.1.1]hept-3-enyl] methanol (HU-308)³⁷ (K_i = 22.7 nM) or (6*aR*,10*aR*)-3-(1,1-dimethylbutyl)-6*a*,7,10,10*a*-tetrahydro-6,6,9-trimethyl-6*H*-dibenzo[*b,d*]pyran (JWH-133)³⁸ (K_i = 3.4 nM). Moreover, the selectivity of compound **43** (CB₁/CB₂ > 3125) for CB₂ receptor was higher than that of JWH-133 (CB₁/CB₂ = 200) or HU-308 (CB₁/CB₂ = 450).

Potency in Functional Assays

Compounds showing high affinity for the CB₂ receptor (K_i values under 160 nM) (**16–18**, **22**, **28**, **31**, **34**, **35**, **37**, **39**, **41**, **42**, **43**, and **44**) were selected for functional evaluation in cAMP determination experiments. To further assess CB₂ receptor activity through a different outcome, GTP γ S binding assays of **34**, **42–44** were performed.

Functional properties of CB₂ ligands (**16–18**, **22**, **28**, **31**, **34**, **35**, **37**, **39**, and **41–44**) were appraised through cAMP assays using HEK293 cells stably expressing hCB₂R and treated with forskolin to activate adenylyl cyclase. Effects of tested compounds on forskolin-stimulated cAMP levels were determined in a preliminary screening at two concentrations, at 200 nM and at 1 μ M (Figure 2). The cannabinoid reference compound, 2-[(1*R*,2*R*,5*R*)-5-hydroxy-2-(3-hydroxypropyl) cyclohexyl]-5-(2-methyloctan-2-yl)phenol (CP55,940)³⁹ was also tested in this assay as reference. Compounds **17**, **18**, **22**, **28**, **34**, **37**, **39**, and **41–44** displayed low to high inhibition of forskolin-stimulated cAMP accumulation at both concentrations. The tested compounds were also screened in normal HEK293 cells at the

same two concentrations to confirm that these effects were CB₂ receptor-mediated (Supporting Information).

Full concentration–response curves were measured to determine IC₅₀ and maximum inhibition values for the most potent compounds (**34** and **41–44**); the other compounds (**17**, **18**, **22**, **28**, **37**, and **39**) behave as partial or weak agonists. As shown in Table 4, **34** and **41–44** are potent CB₂ agonists with IC₅₀ values in the nanomolar range with chromenoisoxazole **43** being the most potent and efficient (IC₅₀ = 4.2 nM).

CB₂ agonist properties of **34** and **42–44** were confirmed by [³⁵S]-GTPγS binding assays performed in commercial CB₂ receptor-containing membranes. The EC₅₀ values obtained from the respective concentration–response curves are collected in Table 4. Agonist potencies of **34** and **42–44** vary from [³⁵S]-GTPγS (EC₅₀: 38.6–539.6 nM) to cAMP experiments (EC₅₀: 4.2–134.0 nM) experiments. However, in both assay types, chromenoisoxazole **43** stood out to be the most potent selective CB₂ receptor ligand of the series.

CB₂ receptor ligands (**16**, **31**, and **35**) that in the preliminary screening exhibited no effect on forskolin-stimulated cAMP accumulation were tested for CB₂R antagonism in cAMP assays. Compounds **16** and **35** were able to antagonize the effect of the cannabinoid agonist CP55,940 (100 nM and 1 μM) at a concentration of 200 nM, whereas **31** behaved as the CP55,940 antagonist only at the highest concentration (Figure 3).

In what concerns the CB₁ receptor activity, only the effect of the new compounds showing the highest affinity for CB₁ receptor (**10b**, **22**, and **42**) was determined. Potencies of **10b**, **22**, and **42** were evaluated through GTPγS binding assays performed in membranes extracted from HEK293 cells stably expressing the human CB₁ receptor (Table 5). Tested compounds, **10b**, **22** and **42**, produced an increase of basal [³⁵S]-GTPγS binding, being **42** at least 10-fold more potent than **10b** and **22**.

Molecular Modeling

During the course of our studies, cannabinoid selectivity and structural patterns led us to select molecules **5**, **7b**, **18**, and **42** for docking studies. Given the high CB₁ selectivity of the chromenopyrazole **5**, it was surprising that the corresponding isoxazole derivative **42** showed high affinity for both cannabinoid receptors. Therefore, we report here docking studies of both compounds (**5** and **42**) in the refined CB₁ and CB₂ active state models. We also considered interesting that the replacement of the hydroxyphenyl by a methoxyphenyl led to full CB₂ selectivity in the chromenopyrazole series. Varying degrees of CB₂ selectivity and affinity were reported in the literature for some classical cannabinoids such as the HU-308³⁷ and methoxy-⁸-THC derivatives.⁴⁰ However, these O-methylations have not been fully explored in terms of interactions with the binding site. Therefore, the CB₁R selective chromenopyrazole **7b** was studied in relation to its methoxy derivative **18** through docking studies.

First, conformational analysis of **5**, **7b**, **18**, and **42** was performed to determine the global minimum energy conformers (Supporting Information). In what concerns the *N-H*-

chromenopyrazole **5**, this pyrazole can exist as a mixture of two tautomeric forms. However, we only considered the N2-*H*-tautomer based on our previous studies concerning annular tautomerism (OH...N and/or NH...O) of hydroxychromenopyrazoles, in which the tautomer OH...N was shown to be the predominant species in solution.⁴¹ We have then calculated the electrostatic potential maps of the minimum energy conformers of **5**, **7b**, **18**, and **42** (Figure 4). The phenolic hydroxyl group was revealed to be the most negative electrostatic potential region (in red) of **5** (CB₁) and **7b** (CB₁). Chromenoisoxazole **42** (CB₁/CB₂) showed two electron rich hot spots (in red) originated by the phenolic hydroxyl group and by the isoxazole nitrogen, the latter being the most electronegative region of the molecule. As expected, the methoxychromenopyrazole **18** (CB₂) displayed a weaker electronegative region due to the low exposure of the free lone pair of electrons of the methylated phenolic oxygen. A positive electrostatic potential at the corresponding region has also been detected for the highly CB₂ selective ligand **43** (Supporting Information).

The global energy minima of **5**, **7b**, **18**, and **42** were docked using a model of the CB₁ and of the CB₂ in their active state (CB₁R*; CB₂R*).⁴² These models include the extracellular and intracellular loops, the N-terminus (truncated in CB₁R) and the C-terminus, including the intracellular helix portion of each receptor, termed Helix 8. Docking studies were performed in the same binding site described for HU210⁴³ in the CB₁R* model and for AM841^{44,45} in the CB₂R* model.

Docking Studies of 5 and 42 in CB₁R*—As illustrated in Figure 5, the energy-minimized hydroxychromenopyrazole **5**/CB₁R* complex shows two main binding site anchoring interactions. The phenolic oxygen of **5** is engaged in a hydrogen bond with K3.28(192) [hydrogen bond (N–O) distance = 2.75 Å and (N–H–O) angle = 151°]. The N1-pyrazole nitrogen establishes a hydrogen bond with serine S7.39(383) [hydrogen bond (N–O) distance = 3.02 Å and (O–H–N) angle = 140°].

Docking **42** in CB₁R* revealed a similar occupation of the binding site with hydrogen bonds involving K3.28(192) [hydrogen bond (N–O) distance = 2.82 Å and (N–H–O) angle = 153°] and S7.39(383) [hydrogen bond (N–O) distance = 2.77 Å and (O–H–N) angle = 130°] as key residues (Figure 5, right). It is interesting to note that an additional hydrogen bond between the pyran oxygen and cysteine C7.42(386) was revealed in the **42**/CB₁R* complex [hydrogen bond (S–O) distance = 3.19 Å and (S–H–O) angle = 167°].

Docking Studies of 5 and 42 in CB₂R*—The CB₂R* model contains a salt bridge between the aspartic acid D275 in the EC-3 loop and lysine K3.28(109). Docking studies of **5** revealed a steric clash between the pyrazole moiety of the structure and the lysine involved in the ionic lock (Figure 6, left) and in agreement with the experimental pharmacological data (K_i (CB₂R) > 40 μM), whereas the energy minimized **42**/CB₂R* complex presents two main interactions (Figure 6, right), a hydrogen bond between the isoxazole nitrogen and K3.28(109) [hydrogen bond (N–O) distance = 2.86 Å and (N–H–O) angle = 157°] and a hydrogen bond involving the phenolic oxygen of **42** and S6.58(268) [hydrogen bond (O–O) distance = 2.63 Å and (O–H–O) angle = 170°].

Docking Studies of 7b and 18 in CB₁R*—The hydroxychromenopyrazole **7b** and the methoxychromenopyrazole **18** were compared at the CB₁R* binding site (Supporting Information). The **7b**/CB₁R* complex presents two hydrogen bonds with K3.28(192) that involve the phenolic oxygen and the pyrazole N1 nitrogen which also forms a hydrogen bond with S7.39(383). Consistent with its poor CB₁ affinity, **18** was unable to form any hydrogen bond with any residue of the receptor. Indeed, the methoxy group of **18** shows steric overlap with the phenylalanine F2.57(170) and the leucine L7.43(387) inducing low accessibility of the lone pairs of electrons of the phenolic oxygen to K3.28(192) (shown in the Supporting Information).

Docking Studies of 7b and 18 in CB₂R*—Figure 7 illustrates the CB₂R* docking studies of **7b** and **18**. As previously shown for the **5**/CB₂R* complex, the hydroxychromenopyrazole **7b** exhibits a steric clash between the pyrazole moiety and the ionic lock formed by D275 and K3.28(109) with an additional major steric overlap with F7.35(281). These findings likely explain the lack of affinity of chromenopyrazole **7b** for the CB₂ receptor. The methoxy derivative **18** displays similar occupation of the binding site; however, **18** adopts a different orientation than the free phenolic hydroxyl ligands **5**, **42**, and **7b**. This orientation enables S6.58(268) to form a hydrogen bond with the pyran oxygen [hydrogen bond (O–O) distance = 3.21 Å and (O–H–O) angle = 110°].

The results obtained with our docking studies in the CB₂R* model reveal the importance of two residues, S6.58(268) and K3.28(109). The serine S6.58 had been previously mentioned in the interactions of the classical cannabinoid AM841⁴⁸ with CB₂R*.⁴⁵ However, the phenolic hydroxyl of AM841 participated in this interaction. In what concerns the lysine K3.28, its importance to classical cannabinoid binding to CB₁R* is well documented,⁴⁹ whereas K3.28 was considered not essential to bind to CB₂R*.⁴⁵ As shown in our docking studies, K3.28 establishes a hydrogen bond with the isoxazole nitrogen in the **42**/CB₂R* complex.

Furthermore, the docking studies suggested that substitution of the hydroxyl phenol of the potent CB₁/CB₂ compound **42** would lead to a selective CB₂ ligand, as was confirmed by the synthesis of **43** which turned out to be the most interesting of the series.

Drug-Like Properties in Silico

Multivariate statistical analysis of a relative large set of 34 physicochemical descriptors calculated on the global minimum energy conformer of the chromenopyrazoles and chromenoisoxazoles **5–44**, cannabinol (CBN), CP55,940, and ⁹-THC has been realized which data were compared to a range of 95% of drugs. The predicted data (Supporting Information) for the chromenoheterocycle derivatives indicated that Lipinski's and Jorgensen's pharmacokinetics rules are followed. One of the physicochemical properties that need to be optimized for cannabinoids is the lipophilicity, as it is an important factor affecting its bioavailability. Therefore, it is predicted that the chromenoisoxazoles **42–44** have a better bioavailability profile compared to that of classical cannabinoids such as ⁹-THC or CBN calculated in the same predictive model. In what concerns the blood–brain barrier, predictive data of the compounds suggest that they can cross this barrier.

Assessment of the Binding of Compounds to Plasma Proteins

Surface plasmon resonance (SPR) experiments were performed with a Biacore X-100 apparatus to study the different binding levels of selected compounds (**14**, **16–18**, **28**, **31**, **35–37**, **39**, and **41–43**) to two plasma proteins, human serum albumin (HSA) and α_1 -acid glycoprotein (AGP). As this experiment had not been previously reported in the literature for cannabinoids, different reference cannabinoid ligands (rimonabant, SR144528,⁵⁰ WIN55,212-2,⁵¹ HU308, CBD, 2-AG, AEA, and CP55,940) were also assessed for comparison. The results (Supporting Information) indicated that **14–16**, **39**, **40**, and **43** could exhibit medium HSA and AGP binding levels suggesting appropriate free drug concentrations in plasma, whereas **18**, **28**, **36**, **37**, and **42** showed very high plasma protein binding that, if any, could be of interest for in vivo retarding effects. The tested reference cannabinoid ligands CBD, 2AG, and AEA showed very high levels of binding to AGP, whereas CBD, 2-AG, and CP55,940 showed high levels of binding to HSA. It has to be kept in mind that cannabinoids are, in general, very lipophilic compounds.

In Vivo Efficacy of **43** in the Acute Inflammatory Phase of a Multiple Sclerosis Animal Model

One of the most promising therapeutic applications of cannabinoids selectively activating the CB₂ receptor is the reduction of neuroinflammatory events.⁵² Thus, we wanted to investigate the potential in vivo of **43** in experimental models reproducing neuroinflammatory conditions. Multiple sclerosis is a complex inflammatory disease that affects the CNS white matter. The Theiler's murine encephalomyelitis virus (TMEV) model is one of the best viral-based models of multiple sclerosis. Intracerebral infection of susceptible inbred mouse strains with TMEV leads to the induction of a late-onset demyelinating disease, termed TMEV-induced demyelinating disease (TMEV-IDD) which is pathologically similar to human multiple sclerosis. The acute inflammatory phase of TMEV-IDD (day 7 post infection) has a strong neuroinflammatory response with the participation of microglial cells as antigen presenting cells of viral antigens. To assess the efficacy of **43**, mice infected with TMEV for 7 consecutive days were injected intraperitoneally with vehicle (10% DMSO in phosphate-buffered saline, PBS) or **43** at a dose of 5 mg/kg. Brain sections of each animal (described in Experimental Section) were analyzed by immunofluorescence staining. Because microglial cell activation plays a pivotal role in TMEV-IDD,³⁵ we analyzed the effect of **43** on the expression of Iba-1, a marker of microglia, in the brain of TMEV-infected mice. As illustrated in Figure 8, fluorescent staining revealed that TMEV-infection increased the intensity of fluorescence of Iba-1+ cells in the brain. Microglia activation was greatly prevented by administration of **43** leading to a significant reduction of the intensity of microglia activation to levels close to those quantified in the control group (Sham, Figure 8). Therefore, we can conclude that administration of **43** significantly reduced microglial activation in TMEV-infected mice that based on previous studies³⁵ should necessarily reduce inflammatory events and improve the neurological status of treated animals.

Compound **43** has been also recently evaluated with positive results in inflammatory models of Huntington's disease that will be published in due time.

CONCLUSIONS

The pharmacological and docking studies carried out with the newly synthesized chromenopyrazoles and -isoxazoles along with our earlier findings allowed us to determine key structural features for CB₂ receptor binding. O-Alkylated chromenopyrazoles led to compounds displaying high to moderate CB₂ affinity and selectivity vs CB₁, whereas replacement of the pyrazole core by an isoxazole led to very potent cannabinoid ligands. Even though different degrees of CB₂ selectivity and affinity were reported in the literature for classical cannabinoids, their binding site interactions have not been fully explored.⁴⁵ The results obtained with our docking studies in the CB₂R* model reveal the importance of two residues, S6.58(268) and K3.28(109). The serine S6.58 that had been previously described as interacting with the phenolic hydroxyl of classical cannabinoid,⁴⁵ established a hydrogen bond with the pyran oxygen and our compounds. The residue K3.28 that was considered not essential for classical cannabinoids to bind to CB₂R*⁴⁵ formed a hydrogen bond with the isoxazole nitrogen that conferred CB₂ affinity to the chromenoisoxazole compared to the corresponding chromenopyrazole. Finally, these studies led to the synthesis of the chromenoisoxazole **43** that was shown to be fully CB₂ selective with a high affinity constant.

Multiple sclerosis is the major immune-mediated, demyelinating and neurodegenerative disease of the central nervous system (CNS). A mixture of ⁹-THC and a cannabidiol oromucosal spray has shown clinical benefit in reducing spasticity symptoms in multiple sclerosis, and it is now licensed for the treatment of multiple sclerosis symptoms. However, there is now abundant experimental evidence that cannabinoids can act as immunomodulators and neuroprotective agents in both in vitro and in vivo models of neurodegeneration.³⁰ In particular, the CB₂ receptor has been associated with the anti-inflammatory and immunomodulatory actions exerted by cannabinoids⁵³ and has been suggested to play a role in multiple sclerosis models.^{54,55} The modulation of the innate immunity including microglia responses to TMEV infection by cannabinoid treatment affected the development and progression of disabilities in the TMEV-IDD model.^{35,56} In this context, compound **43** has been tested in the acute inflammatory phase of the TMEV model. Administration of **43** significantly reduced microglial activation.

EXPERIMENTAL SECTION

Chemistry. General Methods and Materials

Reagents and solvents were purchased from Sigma-Aldrich Co., Fluorochem, Acros Organics, Manchester Organics, or Lab-Scan and were used without further purification or drying. Silica gel 60 F254 (0.2 mm) thin layer plates were purchased from Merck GmbH. Microwave assisted organic synthesis was performed using the microwave reactor Biotage Initiator. Products were purified using flash column chromatography (Merck Silica gel 60, 230–400 mesh) or medium pressure chromatography using Biotage Isolera One with prepacked silica gel columns (Biotage SNAP cartridges). The compounds were characterized by a combination of NMR experiments, HPLC-MS, high-resolution mass spectrometry (HRMS), and elemental analysis. HPLC-MS analysis was performed on a Waters 2695 HPLC system equipped with a photodiode array 2996 coupled to Micromass ZQ 2000 mass spectrometer (ESI-MS), using a reverse-phase column SunFire™ (C-18, 4.6

× 50 mm, 3.5 μm) in a 10 min gradient A, CH₃CN/0.1% formic acid, and B, H₂O/0.1% formic acid visualizing at λ = 254 nm. The flow rate was 1 mL/min. Elemental analyses of the compounds were performed using a LECO CHNS-932 apparatus. Deviations of the elemental analysis results from the calculated one are within ±0.4%. ¹H, ¹³C, HSQC, and HMBC-NMR spectra were recorded on a Bruker 300 (300 and 75 MHz) or a Varian 500 (500 and 126 MHz) at 25 °C. Samples were prepared as solutions in deuterated solvent and referenced to internal nondeuterated solvent peaks. Chemical shifts were expressed in ppm (δ) downfield of tetramethylsilane. Coupling constants are given in hertz (Hz). Melting points were measured on a MP 70 Mettler Toledo apparatus. The synthesis of compounds **2–9** have been previously described by us.³⁴

General Procedure for the Preparation of 10, 12–14—A solution of **4**³⁴ (1 mmol) and the corresponding hydrazine (2.5 mmol) in EtOH was stirred during 4 h at 40 °C. The solvent was evaporated under reduced pressure, and the crude was purified by column chromatography on silica gel.

7-(1,1-Dimethylheptyl)-1,4-dihydro-1-(2-hydroxyethyl)-4,4-dimethylchromeno[4,3-c]pyrazol-9-ol (10a) and 7-(1,1-Dimethyl-heptyl)-2,4-dihydro-2-(2-hydroxyethyl)-4,4-dimethylchrome-no[4,3-c]pyrazol-9-ol (10b): The title compounds were prepared from 2-hydroxyethylhydrazine with column chromatography on silica gel (hexane/EtOAc, 2:3). Compound **10a** was obtained as a white oil (10 mg, 23%). ¹H NMR (300 MHz, CDCl₃) δ: 8.15 (s, 1H, 9-OH), 7.30 (s, 1H, 3-H), 6.62 (d, *J* = 1.6 Hz, 1H, 8-H), 6.53 (d, *J* = 1.6 Hz, 1H, 6-H), 4.29 (t, *J* = 5.7 Hz, 2H, NCH₂CH₂OH), 4.10–4.03 (m, 2H, NCH₂CH₂OH), 1.65 (s, 6H, OC(CH₃)₂), 1.62–1.52 (m, 2H, 2'-H), 1.28 (s, 6H, C(CH₃)₂), 1.25–1.17 (m, 6H, 3'-H, 4'-H, 5'-H), 1.16–1.00 (m, 2H, 6'-H), 0.87 ppm (t, *J* = 6.6 Hz, 3H, 7'-H). ¹³C NMR (75 MHz, CDCl₃) δ: 152.9 (9-C), 152.6 (7-C), 152.4 (5a-C), 143.0 (9b-C), 124.2 (3-C), 120.0 (3a-C), 106.4 (8-C), 106.1 (6-C), 100.8 (9a-C), 76.1 (OC(CH₃)₂), 61.4 (NCH₂CH₂OH), 54.0 (NCH₂CH₂OH), 44.2 (2'-C), 37.8 (C(CH₃)₂), 31.5, 29.7, 24.4 (3'-C, 4'-C, 5'-H), 29.3 (C(CH₃)₂), 28.6 (OC(CH₃)₂), 22.4 (6'-C), 13.8 ppm (7'-C). HPLC-MS: [A, 70 → 95%]. *t*_R: 5.11 min, (95%); MS (ES⁺, *m/z*) 387 [M + H]⁺. Anal. Calcd for C₂₃H₃₄N₂O₃: C 71.47, H 8.87; found, C 71.19, H 9.04. Compound **10b** was obtained as a yellow solid (22 mg, 50%). mp: 93–95 °C. ¹H NMR (300 MHz, CDCl₃) δ: 7.38 (s, 1H, 3-H), 6.63 (d, *J* = 1.8 Hz, 1H, 8-H), 6.50 (d, *J* = 1.9 Hz, 1H, 6-H), 4.63 (t, *J* = 5.0 Hz, 2H, NCH₂CH₂OH), 4.12 (t, *J* = 5.0 Hz, 2H, NCH₂CH₂OH), 1.57 (s, 6H, OC(CH₃)₂), 1.25 (s, 6H, C(CH₃)₂), 1.21–1.16 (m, 8H, 2'-H, 3'-H, 4'-H, 5'-H), 1.13–1.00 (m, 2H, 6'-H), 0.83 ppm (t, *J* = 6.5 Hz, 3H, 7'-H). ¹³C NMR (75 MHz, CDCl₃) δ: 154.4 (9-C), 153.4 (7-C), 150.4 (5a-C), 149.9 (9b-C), 133.7 (3-C), 123.3 (3a-C), 109.3 (6-C), 108.8 (8-C), 102.9 (9a-C), 76.8 (OC(CH₃)₂), 62.1 (NCH₂CH₂OH), 53.5 (NCH₂CH₂OH), 44.6 (2'-C), 38.0 (C(CH₃)₂), 32.0, 30.2, 25.9 (3'-C, 4'-C, 5'-H), 28.9 (OC(CH₃)₂), 27.5 (C(CH₃)₂), 22.9 (6'-C), 14.3 ppm (7'-C); HPLC-MS: [A, 70 → 95%]. *t*_R: 3.93 min, (99%); MS (ES⁺, *m/z*) 387 [M + H]⁺. Anal. Calcd for C₂₃H₃₄N₂O₃: C 71.47, H 8.87; found, C 71.62, H 8.96.

7-(1,1-Dimethylheptyl)-2,4-dihydro-2-hydroxymethyl-4,4-dimethylchromeno[4,3-c]pyrazol-9-ol (11): Formaldehyde (37% in water, 13 μL, 0.17 mmol) was added to chromenopyrazole **5** (20 mg, 0.05 mmol) dissolved in ethanol (2 mL). The mixture was

heated under reflux for 5 h and then cooled down to room temperature. After evaporation of the solvent under reduced pressure, the crude was purified by chromatography on silica gel (hexane/EtOAc, 1:1). Compound **11** was obtained as a white solid (14 mg, 69%). mp: 90–92 °C. ¹H NMR (300 MHz, CDCl₃) δ: 7.35 (s, 1H, 3-H), 6.59 (d, *J* = 1.6 Hz, 1H, 8-H), 6.51 (d, *J* = 1.6 Hz, 1H, 6-H), 5.30 (s, 2H, NCH₂OH), 1.64 (s, 6H, OC(CH₃)₂), 1.61–1.49 (m, 2H, 2'-H), 1.25 (s, 6H, C(CH₃)₂), 1.23–0.94 (m, 6H, 3'-H, 4'-H, 5'-H), 0.81 ppm (t, *J* = 4.8 Hz, 3H, 7'-H). ¹³C NMR (75 MHz, CDCl₃) δ: 151.7 (9-C), 150.6 (7-C), 149.1 (5a-C), 148.2 (9b-C), 127.0 (3-C), 124.7 (3a-C), 110.1 (6-C), 109.3 (8-C), 104.9 (9a-C), 75.4 (OC(CH₃)₂), 65.8 (NCH₂OH), 43.2 (2'-C), 39.5 (C(CH₃)₂), 32.5, 31.6, 25.5 (3'-C, 4'-C, 5'-C), 28.9 (OC(CH₃)₂), 27.4 (C(CH₃)₂), 23.7 (6'-C), 14.7 ppm (7'-C). HPLC-MS: [A, 80 → 95%]. *t*_R: 3.42 min (96%); MS (ES⁺, *m/z*) 373 [M + H]⁺. Anal. Calcd for C₂₂H₃₂N₂O₃: C 70.94, H 8.66; found, C 71.12, H 8.93.

1-(3,5-Difluorophenyl)-7-(1,1-dimethylheptyl)-1,4-dihydro-4,4-dimethylchromenof[4,3-c]pyrazol-9-ol (12): The title compound was prepared from 3,5-difluorophenylhydrazine hydrochloride. Column chromatography on silica gel (hexane/EtOAc, 3:1) afforded **12** as a yellow oil (32 mg, 82%). ¹H NMR (300 MHz, CDCl₃) δ: 7.55 (s, 1H, 3-H), 7.10–6.98 (m, 3H, 2-H_{Ph}, 4-H_{Ph}, 6-H_{Ph}), 6.65 (d, *J* = 1.9 Hz, 1H, 6-H), 6.70 (d, *J* = 1.9 Hz, 1H, 8-H), 1.62 (s, 6H, OC(CH₃)₂), 1.49–1.43 (m, 2H, 2'-H), 1.26 (s, 6H, C(CH₃)₂), 1.19–1.08 (s, 8H, 3'-H, 4'-H, 5'-H, 6'-H), 0.93–0.85 ppm (m, 3H, 7'-H). ¹³C NMR (75 MHz, CDCl₃) δ: 155.2 (9-C), 154.0 (5a-C), 152.6 (7-C), 141.7 (1-C_{Ph}), 136.3 (3-C), 135.7 (3-C_{Ph}), 135.4 (3-C_{Ph}), 134.2 (9b-C), 130.1, 128.7, 126.0 (2-C_{Ph}, 4-C_{Ph}, 6-C_{Ph}), 122.9 (3a-C), 109.3 (6-C), 108.1 (8-C), 103.9 (9a-C), 75.6 (OC(CH₃)₂), 44.0 (2'-C), 38.8 (C(CH₃)₂), 32.6, 31.0, 25.7, 23.2 (3'-C, 4'-C, 5'-C, 6'-C), 28.7 (C(CH₃)₂), 27.4 (OC(CH₃)₂), 15.1 ppm (7'-C). HPLC-MS: [A, 80% → 95%]. *t*_R: 4.22 min (99%). MS (ES⁺, *m/z*) 455 [M + H]⁺. Anal. Calcd for C₂₇H₃₂F₂N₂O₂: C 71.34, H 7.10; found, C 71.02, H 6.95.

7-(1,1-Dimethylheptyl)-1,4-dihydro-1-(3-methoxyphenyl)-4,4-dimethylchromenof[4,3-c]pyrazol-9-ol (13): The title compound was prepared from 3-methoxyphenylhydrazine hydrochloride. Column chromatography on silica gel (hexane/EtOAc, 3:1) afforded **13** as a yellow oil (48 mg, 47%). ¹H NMR (300 MHz, CDCl₃) δ: 7.47 (s, 1H, 3-H), 7.32 (t, *J* = 7.5 Hz, 1H, 5-H_{Ph}), 7.27 (t, *J* = 1.7 Hz, 1H, 2-H_{Ph}), 7.18–7.13 (m, 1H, 6-H_{Ph}), 7.01–6.96 (m, 1H, 4-H_{Ph}), 6.60 (d, *J* = 1.8 Hz, 1H, 6-H), 6.53 (d, *J* = 1.8 Hz, 1H, 8-H), 3.75 (s, 3H, OCH₃), 1.63 (s, 6H, OC(CH₃)₂), 1.60–1.52 (m, 2H, 2'-H), 1.31–1.20 (m, 12H, 3'-H, 4'-H, 5'-H, C(CH₃)₂), 1.16–1.09 (m, 2H, 6'-H), 0.89–0.79 ppm (m, 3H, 7'-H). ¹³C NMR (75 MHz, CDCl₃) δ: 156.1 (9-C), 154.1 (3-C_{Ph}), 150.9 (5a-C), 141.2 (7-C), 138.2 (1-C_{Ph}), 136.2 (3-C), 133.4 (9b-C), 130.2 (5-C_{Ph}), 123.4 (6-C_{Ph}), 122.3 (4-C_{Ph}), 120.3 (3a-C), 109.0 (2-C_{Ph}), 108.6 (6-C), 105.0 (8-C), 103.4 (9a-C), 75.0 (OC(CH₃)₂), 56.3 (OCH₃), 44.8 (2'-C), 38.7 (C(CH₃)₂), 31.7, 30.2, 26.1 (3'-C, 4'-C, 5'-C), 28.9 (C(CH₃)₂), 27.6 (OC(CH₃)₂), 23.0 (6'-C), 14.3 ppm (7'-C). HPLC-MS: [A, 80 → 95%]. *t*_R: 3.81 min (94%). MS (ES⁺, *m/z*) 449 [M + H]⁺. Anal. Calcd for C₂₈H₃₆N₂O₃: C 74.97, H 8.09; found, C 75.06, H 7.78.

1-Cyclohexyl-7-(1,1-dimethylheptyl)-1,4-dihydro-4,4-dimethylchromenof[4,3-c]pyrazol-9-ol (14): Prepared from cyclohexylhydrazine hydrochloride (0.12 g, 0.80 mmol). Column chromatography on silica gel (hexane/EtOAc, 2:1) afforded compound **14** as a pale-

yellow solid (39 mg, 35%). mp: 98–100 °C. ¹H NMR (300 MHz, CDCl₃) δ: 7.38 (s, 1H, 3-H), 6.62 (d, *J* = 1.7 Hz, 1H, 6-H), 6.57 (d, *J* = 1.7 Hz, 1H, 8-H), 4.61–4.52 (m, 1H, H_a), 1.86–1.80 (m, 4H, H_b and H_f), 1.76–1.69 (m, 6H, H_c, H_d, H_e), 1.64 (s, 6H, OC(CH₃)₂), 1.49–1.44 (m, 2H, 2'-H), 1.24 (s, 6H, C(CH₃)₂), 1.19–1.08 (m, 8H, 3'-H, 4'-H, 5'-H, 6'-H), 0.92–0.86 ppm (m, 3H, 7'-H). ¹³C NMR (75 MHz, CDCl₃) δ: 152.8 (9-C), 151.6 (7-C), 149.9 (5a-C), 134.8 (9b-C), 130.6 (3-C), 125.3 (3a-C), 109.3 (8-C), 106.1 (6-C), 103.2 (9a-C), 75.7 (OC(CH₃)₂), 50.3 (C), 43.1 (2'-C), 38.2 (C(CH₃)₂), 32.6 (C_b, C_f), 31.6, 31.0, 24.0, 22.8 (3'-C, 4'-C, 5'-C, 6'-C), 28.9 (C(CH₃)₂), 27.7 (OC(CH₃)₂), 26.9, 26.3 (C_c, C_d, C_e), 14.7 ppm (7'-C). HPLC-MS: [A, 80 → 95%]. *t*_R: 5.02 min, (97%). MS (ES⁺, *m/z*) 426 [M + H]⁺. Anal. Calcd for C₂₇H₄₀N₂O₂: C 76.37, H 9.50; found, C 76.11, H 9.74.

General Procedure for the Preparation of 15–39—A solution of the selected hydroxychromenopyrazole from **5–9** (1 equiv) in anhydrous THF was added dropwise to a precooled suspension of sodium hydride (1.6 equiv) in anhydrous THF under nitrogen atmosphere. The resulting yellow solution was stirred for 10 min at rt. Then, the corresponding alkylating agent (3–5 equiv) was rapidly added. The reaction mixture was refluxed for 1–12 h. The crude was diluted with diethyl ether or EtOAc, filtered, concentrated under vacuum, and purified on column chromatography on silica gel.

7-(1,1-Dimethylheptyl)-2,4-dihydro-9-methoxy-4,4-dimethylchromeno[4,3-c]pyrazole (15): The title compound was prepared from **5** and iodomethane. Column chromatography on silica gel (hexane/EtOAc, 3:1) afforded **15** as a yellow oil (21 mg, 40%). ¹H NMR (300 MHz, CDCl₃) δ: 8.13–8.09 (br s, 1H, NH), 7.31 (d, *J* = 1.5 Hz, 1H, 6-H), 7.19 (d, *J* = 1.5 Hz, 8-H), 6.74 (s, 1H, 3-H), 3.95 (s, 3H, OCH₃), 1.69–1.60 (br s, 6H, OC(CH₃)₂), 1.60–1.56 (m, 2H, 2'-H), 1.39 (s, 6H, C(CH₃)₂), 1.25–1.22 (m, 6H, 3'-H, 4'-H, 5'-H), 1.17–1.08 (m, 2H, 6'-H), 0.81 ppm (t, *J* = 6.7 Hz, 3H, 7'-H). ¹³C NMR (75 MHz, CDCl₃) δ: 157.0 (9-C), 155.4 (5a-C), 154.1 (7-C), 143.2 (9b-C), 125.6 (3-C), 120.1 (3a-C), 108.0 (8-C), 107.5 (6-C), 102.3 (9a-C), 76.8 (OC(CH₃)₂), 49.6 (OCH₃), 43.7 (2'-C), 40.2 (C(CH₃)₂), 37.2, 34.7, 24.6 (3'-C, 4'-C, 5'-C), 29.1 (C(CH₃)₂), 28.3 (OC(CH₃)₂), 22.7 (6'-C), 15.1 ppm (7'-C). HPLC-MS: [A, 80% → 95%]. *t*_R: 5.41 min, (97%); MS (ES⁺, *m/z*) 357 [M + H]⁺. Anal. Calcd for C₂₂H₃₂N₂O₂: C 74.12, H 9.05; found, C 74.35, H 8.87.

7-(1,1-Dimethylheptyl)-2,4-dihydro-9-methoxy-2,4,4-trimethylchromeno[4,3-c]pyrazole (16): The title compound was prepared from **6b** and iodomethane. Column chromatography on silica gel (hexane/EtOAc, 2:1) afforded **16** as a white solid (17 mg, 68%). mp: 85–87 °C. ¹H NMR (300 MHz, CDCl₃) δ: 7.63 (s, 1H, 3-H), 6.91 (d, *J* = 1.8 Hz, 1H, 6-H), 6.76 (d, *J* = 1.8 Hz, 1H, 8-H), 4.02 (s, 3H, NCH₃), 3.90 (s, 3H, OCH₃), 1.59 (s, 6H, OC(CH₃)₂), 1.45–1.36 (m, 2H, 2'-H), 1.30 (s, 6H, C(CH₃)₂), 1.2–1.13 (m, 6H, 3'-H, 4'-H, 5'-H), 1.10–1.03 (m, 2H, 6'-H), 0.87 ppm (t, *J* = 7.0 Hz, 3H, 7'-H). ¹³C NMR (75 MHz, CDCl₃) δ: 153.2 (9-C), 152.6 (5a-C), 151.8 (7-C), 142.1 (9b-C), 124.3 (3-C), 122.0 (3a-C), 109.5 (6-C), 105.7 (8-C), 103.1 (9a-C), 76.2 (OC(CH₃)₂), 57.0 (OCH₃), 45.3 (NCH₃), 39.2 (2'-C), 37.8 (C(CH₃)₂), 32.0, 31.3, 25.3 (3'-C, 4'-C, 5'-C), 29.5 (C(CH₃)₂), 27.8 (OC(CH₃)₂), 23.5 (6'-C), 13.8 ppm (7'-C). HPLC-MS: [A, 80% → 95%]. *t*_R: 3.58 min (99%). MS (ES⁺, *m/z*) 371 [M + H]⁺. Anal. Calcd for C₂₃H₃₄N₂O₂: C 74.55, H 9.25; found, C 74.89, H 8.96.

7-(1,1-Dimethylheptyl)-1-ethyl-1,4-dihydro-9-methoxy-4,4-dimethylchromeno[4,3-c]pyrazole (17): The title compound was prepared from **6b** and iodomethane. Column chromatography on silica gel (hexane/EtOAc, 3:1) afforded **17** as a white solid (13 mg, 52%). mp: 90–91 °C. ¹H NMR (300 MHz, CDCl₃) δ: 7.34 (s, 1H, 3-H), 6.70 (d, *J* = 1.5 Hz, 2H, 6-H), 6.52 (d, *J* = 1.5 Hz, 1H, 8-H), 4.42 (q, *J* = 7.9 Hz, 2H, NCH₂CH₃), 3.81 (s, 3H, OCH₃), 1.60 (s, 6H, OC(CH₃)₂), 1.54–1.50 (m, 2H, 2'-H), 1.45 (t, *J* = 7.9 Hz, 3H, NCH₂CH₃), 1.31 (s, 6H, C(CH₃)₂), 1.24–1.19 (br s, 8H, 3'-H, 4'-H, 5'-H, 6'-H), 0.86 ppm (t, *J* = 8.0 Hz, 3H, 7'-H). ¹³C NMR (75 MHz, CDCl₃) δ: 153.0 (9-C), 152.6 (5a-C), 150.4 (7-C), 132.3 (3-C), 131.7 (9b-C), 121.9 (3a-C), 109.0 (8-C), 105.3 (6-C), 101.1 (9a-C), 76.8 (OC(CH₃)₂), 54.5 (OCH₃), 49.6 (NCH₂CH₃), 43.9 (2'-C), 38.4 (C(CH₃)₂), 31.8, 30.5, 26.0 (3'-C, 4'-C, 5'-C), 28.7 (C(CH₃)₂), 26.9 (OC(CH₃)₂), 22.9 (6'-C), 15.8 (NCH₂CH₃), 14.6 ppm (7'-C). HPLC-MS: [A, 15% - 95%]. *t*_R: 5.81 min (98%). MS (ES⁺, *m/z*) 385 [M + H]⁺. Anal. Calcd for C₂₄H₃₆N₂O₂: C 74.96, H 9.44; found, C 74.57, H 9.25.

7-(1,1-Dimethylheptyl)-2-ethyl-2,4-dihydro-9-methoxy-4,4-dimethylchromeno[4,3-c]pyrazole (18): The title compound was prepared from **7b** and iodomethane. Column chromatography on silica gel (hexane/EtOAc, 1:1) afforded **18** as a white solid (20 mg, 77%). mp: 87–88 °C. ¹H NMR (300 MHz, CDCl₃) δ: 7.09 (s, 1H, 3-H), 6.50 (d, *J* = 1.3 Hz, 8-H), 6.37 (s, 1H, *J* = 1.3 Hz, 6-H), 4.19 (q, 2H, *J* = 7.2 Hz, NCH₂CH₃), 3.90 (s, 3H, OCH₃), 1.64 (s, 6H, OC(CH₃)₂), 1.57–1.54 (br s, 2H, 2'-H), 1.53 (t, 3H, *J* = 7.6 Hz, NCH₂CH₃), 1.27 (s, 6H, C(CH₃)₂), 1.20–1.11 (m, 6H, 3'-H, 4'-H, 5'-H), 1.09–1.04 (br s, 2H, 6'-H), 0.83 ppm (t, *J* = 7.8 Hz, 3H, 7'-H). ¹³C NMR (75 MHz, CDCl₃) δ: 155.3 (9-C), 154.0 (5a-C), 153.8 (7-C), 143.7 (9b-C), 128.2 (3-C), 126.1 (3a-C), 107.4 (6-C), 106.8 (8-C), 103.7 (9a-C), 78.0 (OC(CH₃)₂), 56.8 (OCH₃), 47.3 (NCH₂CH₃), 45.7 (2'-C), 39.0 (C(CH₃)₂), 32.3, 31.1, 25.7 (3'-C, 4'-C, 5'-C), 29.1 (C(CH₃)₂), 27.4 (OC(CH₃)₂), 23.3 (6'-C), 16.2 (NCH₂CH₃), 14.0 ppm (7'-C). HPLC-MS: [A, 80%–95%]. *t*_R: 3.95 min (99%). MS (ES⁺, *m/z*) 385 [M + H]⁺. Anal. Calcd for C₂₄H₃₆N₂O₂: C 74.96, H 9.44; found, C 75.02, H 9.18.

1-(3,4-Dichlorophenyl)-7-(1,1-dimethylheptyl)-1,4-dihydro-9-methoxy-4,4-dimethylchrome-no[4,3-c]pyrazole (19): The title compound was prepared from **8** and iodomethane. Column chromatography on silica gel (hexane/EtOAc, 1:1) afforded **19** as a yellow oil (11 mg, 47%). ¹H NMR (300 MHz, CDCl₃) δ: 7.81 (d, *J* = 1.9 Hz, 1H, 2-H_{Ph}), 7.72 (s, 1H, 3-H), 7.49 (d, *J* = 7.8 Hz, 1H, 5-H_{Ph}), 7.37 (dd, *J* = 7.8 Hz, *J* = 1.9 Hz, 1H, 6-H_{Ph}), 6.74 (d, *J* = 1.4 Hz, 1H, 6-H), 6.30 (d, *J* = 1.4 Hz, 1H, 8-H), 3.28 (s, 3H, OCH₃), 1.72 (s, 6H, OC(CH₃)₂), 1.68–1.60 (m, 2H, 2'-H), 1.39 (s, 6H, C(CH₃)₂), 1.27–1.18 (m, 6H, 3'-H, 4'-H, 5'-H), 1.12–1.08 (br s, 2H, 6'-H), 0.91 ppm (t, *J* = 7.1 Hz, 3H, 7'-H). ¹³C NMR (75 MHz, CDCl₃) δ: 154.2 (9-C), 153.8 (5a-C), 152.1 (7-C), 143.1 (1-C_{Ph}), 135.7 (3-C), 134.2 (3-C_{Ph}), 132.6 (9b-C), 130.8 (4-C_{Ph}), 126.3 (5-C_{Ph}), 125.9 (2-C_{Ph}), 124.0 (6-C_{Ph}), 120.1 (3a-C), 109.3 (6-C), 108.4 (8-C), 103.5 (9a-C), 76.1 (OC(CH₃)₂), 54.9 (OCH₃), 43.5 (2'-C), 39.0 (C(CH₃)₂), 33.9, 32.3, 26.8 (3'-C, 4'-C, 5'-C), 28.3 (C(CH₃)₂), 27.1 (OC(CH₃)₂), 22.7 (6'-C), 14.0 ppm (7'-C). HPLC-MS: [A, 80% → 95%]. *t*_R: 11.13 min (95%). MS (ES⁺, *m/z*) 501 [M + H]⁺. Anal. Calcd for C₂₈H₃₄Cl₂N₂O₂: C 67.06, H 6.83; found, C 66.79, H 6.55.

1-(2,4-Dichlorophenyl)-7-(1,1-dimethylheptyl)-1,4-dihydro-9-methoxy-4,4-

dimethylchrome-no[4,3-c]pyrazole (20): The title compound was prepared from **9** and iodomethane. Column chromatography on silica gel (hexane/EtOAc, 1:1) afforded **20** as an orange oil (12 mg, 50%). ¹H NMR (300 MHz, CDCl₃) δ: 7.51 (s, 1H, 3-H), 7.47 (d, *J* = 2.0 Hz, 1H, 3-H_{Ph}), 7.35 (dd, *J* = 2.0 Hz, *J* = 8.1 Hz, 1H, 5-H_{Ph}), 7.38 (d, *J* = 8.1 Hz, 1H, 6-H_{Ph}), 6.60 (d, *J* = 1.7 Hz, 1H, 6-H), 6.28 (d, *J* = 1.7 Hz, 1H, 8-H), 3.21 (s, 3H, OCH₃), 1.59 (s, 6H, OC(CH₃)₂), 1.52–1.46 (m, 2H, 2'-H), 1.30 (s, 6H, C(CH₃)₂), 1.19–1.07 (m, 6H, 3'-H, 4'-H, 5'-H), 1.07–1.02 (br s, 2H, 6'-H), 0.79 ppm (t, *J* = 7.0 Hz, 3H, 7'-H). ¹³C NMR (75 MHz, CDCl₃) δ: 157.0 (9-C), 156.3 (5a-C), 155.8 (7-C), 141.7 (1-C_{Ph}), 136.1 (2-C_{Ph}), 135.5 (4-C_{Ph}), 133.9 (3-C), 131.2 (9b-C), 130.8 (3-C_{Ph}), 129.7 (5-C_{Ph}), 128.3 (6-C_{Ph}), 122.9 (3a-C), 109.7 (6-C), 105.2 (8-C), 103.1 (9a-C), 77.4 (OC(CH₃)₂), 56.0 (OCH₃), 43.6 (2'-C), 38.5 (C(CH₃)₂), 33.1, 31.7, 26.4 (3'-C, 4'-C, 5'-C), 29.2 (C(CH₃)₂), 27.9 (OC(CH₃)₂), 24.3 (6'-C), 13.9 ppm (7'-C). HPLC-MS: [A, 80% → 95%]. *t*_R: 9.17 min (98%). MS (ES⁺, *m/z*) 501 [M + H]⁺. Anal. Calcd for C₂₈H₃₄Cl₂N₂O₂: C 67.06, H 6.83; found, C 66.85, H 7.02.

1-(3,4-Dichlorophenyl)-7-(1,1-dimethylheptyl)-9-ethoxy-1,4-dihydro-4,4-

dimethylchrome-no[4,3-c]pyrazole (21): The title compound was prepared from **8** and iodoethane. Column chromatography on silica gel (hexane/EtOAc, 3:1) afforded **21** as a yellow oil (8 mg, 39%). ¹H NMR (300 MHz, CDCl₃) δ: 7.75 (d, *J* = 1.5 Hz, 1H, 2-H_{Ph}), 7.63 (s, 1H, 3-H), 7.41 (d, *J* = 7.2 Hz, 1H, 5-H_{Ph}), 7.29 (dd, *J* = 7.2 Hz, *J* = 1.5 Hz, 1H, 6-H_{Ph}), 6.60 (d, *J* = 1.6 Hz, 1H, 6-H), 6.41 (d, *J* = 1.6 Hz, 1H, 8-H), 3.72 (q, *J* = 7.3 Hz, 2H, OCH₂CH₃), 1.67 (s, 6H, OC(CH₃)₂), 1.55–1.49 (m, 2H, 2'-H), 1.34 (s, 6H, C(CH₃)₂), 1.29–1.20 (m, 6H, 3'-H, 4'-H, 5'-H), 1.16–1.13 (br s, 2H, 6'-H), 1.01 (t, *J* = 7.3 Hz, 3H, OCH₂CH₃), 0.85 ppm (t, *J* = 6.9 Hz, 3H, 7'-H). ¹³C NMR (75 MHz, CDCl₃) δ: 155.4 (9-C), 154.7 (5a-C), 153.5 (7-C), 142.9 (1-C_{Ph}), 134.6 (3-C), 133.1 (3-C_{Ph}), 131.8 (9b-C), 130.6 (4-C_{Ph}), 127.1 (5-C_{Ph}), 126.6 (2-C_{Ph}), 123.1 (6-C_{Ph}), 110.2 (6-C), 106.4 (8-C), 105.8 (9a-C), 76.0 (OC(CH₃)₂), 63.2 (OCH₃), 44.7 (2'-C), 39.8 (C(CH₃)₂), 33.7, 32.0, 27.5 (3'-C, 4'-C, 5'-C), 30.6 (C(CH₃)₂), 28.2 (OC(CH₃)₂), 23.0 (6'-C), 14.2 (OCH₂CH₃), 13.9 ppm (7'-C). HPLC-MS: [iso 95%–5%]. *t*_R: 5.57 min (95%). MS (ES⁺, *m/z*) 515 [M + H]⁺. Anal. Calcd for C₂₉H₃₆Cl₂N₂O₂: C 67.57, H 7.04; found, C 67.23, H 6.89.

9-Benzyloxy-2,4-dihydro-7-(1,1-dimethylheptyl)-4,4-dimethylchromeno[4,3-c]pyrazole (22):

The title compound was prepared from **5** and benzyl bromide. Column chromatography on silica gel (hexane/EtOAc, 3:1) afforded **22** as a yellow solid (5 mg, 41%). mp: 110–112 °C. ¹H NMR (300 MHz, CDCl₃) δ: 7.55–7.29 (m, 5H, 2-H_{Bn}, 3-H_{Bn}, 4-H_{Bn}, 5-H_{Bn}, 6-H_{Bn}), 7.16 (s, 1H, 3-H), 6.62 (d, *J* = 1.5 Hz, 1H, 6-H), 6.57 (d, *J* = 1.5 Hz, 1H, 8-H), 5.18 (s, 2H, OCH₂), 1.64 (s, 6H, OC(CH₃)₂), 1.58–1.48 (m, 2H, 2'-H), 1.25 (s, 6H, C(CH₃)₂), 1.22–1.12 (m, 6H, 3'-H, 4'-H, 5'-H), 1.12–0.96 (m, 2H, 6'-H), 0.90–0.79 ppm (m, 3H, 7'-H). ¹³C NMR (75 MHz, CDCl₃) δ: 157.0 (9-C), 155.2 (5a-C), 153.7 (7-C), 142.5 (9b-C), 139.6 (1-C_{Bn}), 134.8 (3-C), 129.3, 128.1, 127.5 (2-C_{Bn}, 3-C_{Bn}, 4-C_{Bn}, 5-C_{Bn}, 6-C_{Bn}), 124.3 (3a-C), 111.4 (6-C), 108.6 (8-C), 106.3 (9a-C), 75.7 (OC(CH₃)₂), 71.3 (OCH₂), 43.1 (2'-C), 39.4 (C(CH₃)₂), 32.8, 30.6, 25.8 (3'-C, 4'-C, 5'-C), 28.2 (C(CH₃)₂), 27.3 (OC(CH₃)₂), 23.9 (6'-C), 15.1 ppm (7'-C); ppm (7'-C). HPLC-MS: [iso 95%–5%]. *t*_R: 2.25 min (95%). MS (ES⁺, *m/z*) 433 [M + H]⁺. Anal. Calcd for C₂₈H₃₆N₂O₂: C 77.74, H 8.39; found, C 77.92, H 8.16.

9-Benzyloxy-7-(1,1-dimethylheptyl)-2,4-dihydro-2,4,4-trimethylchromeno[4,3-c]pyrazole (23): The title compound was prepared from **6b** and benzyl bromide. Column chromatography on silica gel (hexane/EtOAc, 2:1) afforded **23** as a pale yellow oil (12 mg, 96%). ¹H NMR (300 MHz, CDCl₃) δ: 7.71 (d, *J* = 7.0 Hz, 2H, 2-H_{Bn}, 6-H_{Bn}), 7.41–7.36 (m, 2H, 3-H_{Bn}, 5-H_{Bn}), 7.31–7.26 (m, 1H, 4-H_{Bn}), 7.11 (s, 1H, 3-H), 6.58 (d, *J* = 1.3 Hz, 1H, 6-H), 6.50 (d, *J* = 1.3 Hz, 1H, 8-H), 5.92 (s, 2H, OCH₂), 3.98 (s, 3H, NCH₃), 1.56 (s, 6H, OC(CH₃)₂), 1.50–1.44 (m, 2H, 2'-H), 1.22 (s, 6H, C(CH₃)₂), 1.16–1.11 (m, 6H, 3'-H, 4'-H, 5'-H), 1.05–0.99 (br s, 2H, 6'-H), 0.81 ppm (t, *J* = 8.0 Hz, 3H, 7'-H). ¹³C NMR (75 MHz, CDCl₃) δ: 154.3 (9-C), 153.8 (5a-C), 151.2 (7-C), 141.0 (9b-C), 137.8 (1-C_{Bn}), 128.1 (3-C_{Bn}, 5-C_{Bn}), 127.1 (4-C_{Bn}), 126.9 (2-C_{Bn}, 6-C_{Bn}), 123.2 (3-C), 122.1 (3a-C), 108.9 (6-C), 105.7 (8-C), 104.9 (9a-C), 75.5 (OC(CH₃)₂), 70.6 (OCH₂), 44.5 (NCH₃), 39.0 (2'-C), 37.9 (C(CH₃)₂), 31.7, 29.8, 24.5 (3'-C, 4'-C, 5'-C), 28.9 (C(CH₃)₂), 28.7 (OC(CH₃)₂), 22.5 (6'-C), 14.0 ppm (7'-C). HPLC-MS: [iso 95%–5%]. *t*_R: 2.47 min (99%). MS (ES⁺, *m/z*) 447 [M + H]⁺. Anal. Calcd for C₂₉H₃₈N₂O₂: C 77.99, H 8.58; found, C 77.65, H, 8.81.

9-Benzyloxy-7-(1,1-dimethylheptyl)-1-ethyl-1,4-dihydro-4,4-dimethylchromeno[4,3-c]pyrazole (24): The title compound was prepared from **7a** and benzyl bromide. Column chromatography on silica gel (hexane/EtOAc, 2:1) afforded **24** as a yellow oil (14 mg, 70%). ¹H NMR (300 MHz, CDCl₃) δ: 7.78 (d, *J* = 7.1 Hz, 2H, 2-H_{Bn}, 6-H_{Bn}), 7.49–7.45 (m, 2H, 3-H_{Bn}, 5-H_{Bn}), 7.38–7.33 (m, 1H, 4-H_{Bn}), 7.30 (s, 1H, 3-H), 6.58 (d, *J* = 1.9 Hz, 1H, 6-H), 6.50 (d, *J* = 1.9 Hz, 1H, 8-H), 5.45 (s, 2H, OCH₂), 4.38 (q, *J* = 7.5 Hz, 2H, NCH₂CH₃), 1.63 (s, 6H, OC(CH₃)₂), 1.59–1.55 (br s, 2H, 2'-H), 1.49 (t, 3H, *J* = 7.5 Hz, NCH₂CH₃), 1.29 (s, 6H, C(CH₃)₂), 1.22–1.13 (m, 6H, 3'-H, 4'-H, 5'-H), 1.10–1.02 (m, 2H, 6'-H), 0.90 ppm (t, *J* = 6.7 Hz, 3H, 7'-H). ¹³C NMR (75 MHz, CDCl₃) δ: 152.5 (9-C), 151.9 (5a-C), 150.6 (7-C), 141.0 (9b-C), 138.5 (1-C_{Bn}), 129.2 (3-C_{Bn}, 5-C_{Bn}), 127.0 (4-C_{Bn}), 125.3 (2-C_{Bn}, 6-C_{Bn}), 123.1 (3-C), 121.9 (3a-C), 108.1 (6-C), 106.5 (8-C), 103.9 (9a-C), 74.9 (OC(CH₃)₂), 71.5 (OCH₂), 48.3 (NCH₂CH₃), 45.8 (2'-C), 39.4 (C(CH₃)₂), 32.1, 30.8, 25.6 (3'-C, 4'-C, 5'-C), 29.3 (C(CH₃)₂), 28.1 (OC(CH₃)₂), 23.0 (6'-C), 14.9 (NCH₂CH₃), 13.7 ppm (7'-C). HPLC-MS: [iso 95%–5%]. *t*_R: 3.28 min (96%). MS (ES⁺, *m/z*) 461 [M + H]⁺. Anal. Calcd for C₃₀H₄₀N₂O₂: C 78.22, H 8.75; found, C 77.98, H 9.06.

9-Benzyloxy-7-(1,1-dimethylheptyl)-2-ethyl-2,4-dihydro-4,4-dimethylchromeno[4,3-c]pyrazole (25): The title compound was prepared from **7b** and benzyl bromide. Column chromatography on silica gel (hexane/EtOAc, 3:1) afforded **25** as a white oil (14 mg, 81%). ¹H NMR (300 MHz, CDCl₃) δ: 7.76 (d, *J* = 7.1 Hz, 2H, 2-H_{Bn}, 6-H_{Bn}), 7.40–7.37 (m, 2H, 3-H_{Bn}, 5-H_{Bn}), 7.32–7.27 (m, 1H, 4-H_{Bn}), 7.15 (s, 1H, 3-H), 6.60 (d, *J* = 1.7 Hz, 1H, 6-H), 6.59 (d, *J* = 1.7 Hz, 1H, 8-H), 5.28 (s, 2H, OCH₂), 4.24 (q, *J* = 7.3 Hz, 2H, NCH₂CH₃), 1.63–1.58 (m, 11H, OC(CH₃)₂, 2'-H, NCH₂CH₃), 1.25 (s, 6H, C(CH₃)₂), 1.20–1.07 (m, 6H, 3'-H, 4'-H, 5'-H), 1.08–0.91 (m, 2H, 6'-H), 0.83 ppm (t, *J* = 6.9 Hz, 3H, 7'-H). ¹³C NMR (75 MHz, CDCl₃) δ: 154.4 (9-C), 153.8 (5a-C), 151.1 (7-C), 140.8 (9b-C), 137.9 (1-C_{Bn}), 128.1 (3-C_{Bn}, 5-C_{Bn}), 127.1 (4-C_{Bn}), 126.9 (2-C_{Bn}, 6-C_{Bn}), 121.7 (3-C), 121.0 (3a-C), 109.0 (6-C), 105.9 (8-C), 104.7 (9a-C), 75.6 (OC(CH₃)₂), 70.5 (OCH₂), 47.1 (NCH₂CH₃), 44.6 (2'-C), 38.0 (C(CH₃)₂), 31.7, 29.9, 24.6 (3'-C, 4'-C, 5'-C), 28.9 (C(CH₃)₂), 27.8 (OC(CH₃)₂), 22.6 (6'-C), 15.4 (NCH₂CH₃), 14.1 ppm (7'-C). HPLC-MS: [iso 95%–5%].

t_R : 2.67 min (99%). MS (ES⁺, m/z) 461 [M + H]⁺. Anal. Calcd for C₃₀H₄₀N₂O₂: C 78.22, H 8.75; found, C 78.50, H 8.97.

9-Benzyloxy-1-(3,4-dichlorophenyl)-7-(1,1-dimethylheptyl)-1,4-dihydro-4,4-dimethylchromeno[4,3-c]pyrazole (26): The title compound was prepared from **8** and benzyl bromide. Column chromatography on silica gel (hexane/EtOAc, 3:1) afforded **26** as a pale yellow oil (13 mg, 75%). ¹H NMR (300 MHz, CDCl₃) δ : 7.44 (s, 1H, 3-H), 7.32–7.19 and 7.12–6.95 (m and m, 4H and 4H, 2-H_{Bn}, 3-H_{Bn}, 4-H_{Bn}, 5-H_{Bn}, 6-H_{Bn}, 2-H_{Ph}, 5-H_{Ph}, 6-H_{Ph}), 6.66 (d, J = 1.6 Hz, 1H, 6-H), 6.44 (d, J = 1.6 Hz, 1H, 8-H), 4.53 (s, 2H, OCH₂), 1.55 (s, 8H, OC(CH₃)₂, 2'-H), 1.20 (s, 6H, C(CH₃)₂), 1.14–1.10 (m, 6H, 3'-H, 4'-H, 5'-H), 1.07–0.88 (m, 2H, 6'-H), 0.83–0.72 ppm (m, 3H, 7'-H). ¹³C NMR (75 MHz, CDCl₃) δ : 154.0 (9-C), 153.3 (5a-C), 152.9 (7-C), 142.0 (9b-C), 135.5 (3-C), 134.9, 132.5, 131.7, 130.2, 129.4, 128.4, 128.2, 128.0, 127.8, 127.6, 127.4, 125.2 (1-C_{Bn}, 2-C_{Bn}, 3-C_{Bn}, 4-C_{Bn}, 5-C_{Bn}, 6-C_{Bn}, 1-C_{Ph}, 2-C_{Ph}, 3-C_{Ph}, 4-C_{Ph}, 5-C_{Ph}, 6-C_{Ph}), 124.7 (3a-C), 122.2 (9a-C), 109.6 (6-C), 103.6 (8-C), 76.2 (OC(CH₃)₂), 70.0 (OCH₂), 44.4 (2'-C), 38.2 (C(CH₃)₂), 31.7, 29.9, 24.6 (3'-C, 4'-C, 5'-C), 28.7 (C(CH₃)₂), 27.2 (OC(CH₃)₂), 22.6 (6'-C), 14.1 ppm (7'-C). HPLC-MS: [iso 95%–5%]. t_R : 6.44 min (94%). MS (ES⁺, m/z) 577 [M + H]⁺. Anal. Calcd for C₃₄H₃₈Cl₂N₂O₂: C 70.70, H 6.63; found, C 70.82, H 6.57.

9-Benzyloxy-1-(2,4-dichlorophenyl)-7-(1,1-dimethylheptyl)-1,4-dihydro-4,4-dimethyl-9-methoxychromeno[4,3-c]pyrazole (27): The title compound was prepared from **9** and benzyl bromide. Column chromatography on silica gel (hexane/EtOAc, 3:1) afforded **27** as an orange oil (13 mg, 61%). ¹H NMR (300 MHz, CDCl₃) δ : 7.55 (s, 1H, 3-H), 7.36–7.27 (m, 4H, 2-H_{Bn}, 3-H_{Bn}, 5-H_{Bn}, 6-H_{Bn}), 7.15 (d, J = 2.3 Hz, 1H, 3-H_{Ph}), 7.13–7.02 (m, 2H, 6-H_{Ph}, 4-H_{Bn}), 6.97 (dd, J = 8.5, 2.3 Hz, 1H, 5-H_{Ph}), 6.65 (d, J = 1.6 Hz, 1H, 6-H), 6.35 (d, J = 1.6 Hz, 1H, 8-H), 4.53 (s, 2H, OCH₂), 1.64 (s, 6H, OC(CH₃)₂), 1.52–1.36 (m, 2H, 2'-H), 1.22 (s, 6H, C(CH₃)₂), 1.20–1.09 (m, 6H, 3'-H, 4'-H, 5'-H), 1.03–0.89 (m, 2H, 6'-H), 0.88–0.79 ppm (m, 3H, 7'-H). ¹³C NMR (75 MHz, CDCl₃) δ : 154.1 (9-C), 153.7 (5a-C), 153.3 (7-C), 140.3 (9b-C), 136.8 (3-C), 135.2, 134.8, 133.9, 131.7, 131.7, 129.8, 128.9, 128.8, 128.5, 128.3, 127.7, 127.1 (1-C_{Bn}, 2-C_{Bn}, 3-C_{Bn}, 4-C_{Bn}, 5-C_{Bn}, 6-C_{Bn}, 1-C_{Ph}, 2-C_{Ph}, 3-C_{Ph}, 4-C_{Ph}, 5-C_{Ph}, 6-C_{Ph}), 123.7 (9a-C), 109.7 (6-C), 104.2 (8-C), 77.6 (OC(CH₃)₂), 70.6 (OCH₂), 44.8 (2'-C), 38.5 (C(CH₃)₂), 32.1, 30.2, 24.9 (3'-C, 4'-C, 5'-C), 29.1 (C(CH₃)₂), 27.9 (OC(CH₃)₂), 23.0 (6'-C), 14.5 ppm (7'-C). HPLC-MS: [iso 95%–5%]. t_R : 4.12 min (94%). MS (ES⁺, m/z) 577 [M + H]⁺. Anal. Calcd for C₃₄H₃₈Cl₂N₂O₂: C 70.70, H 6.63; found, C 70.95, H 6.49.

7-(1,1-Dimethylheptyl)-2,4-dihydro-9-(3-hydroxypropoxy)-4,4-dimethylchromeno[4,3-c]pyrazole (28): The title compound was prepared from **5** and 3-bromo-1-propanol. Column chromatography on silica gel (hexane/EtOAc, 1:1) afforded **28** as a white solid (55 mg, 47%). mp: 82–84 °C. ¹H NMR (300 MHz, CDCl₃) δ : 8.28–8.21 (br s, 1H, NH), 7.18 (s, 1H, 3-H), 6.58 (d, J = 1.6 Hz, 1H, 6-H), 6.49 (d, J = 1.6 Hz, 1H, 8-H), 4.29 (t, J = 6.5 Hz, 2H, OCH₂CH₂CH₂OH), 3.67 (t, J = 6.3 Hz, 2H, OCH₂CH₂CH₂OH), 2.13 (p, J = 6.3 Hz, 2H, OCH₂CH₂CH₂OH), 1.61 (s, 6H, OC(CH₃)₂), 1.59–1.45 (m, 2H, 2'-H), 1.25 (s, 6H, C(CH₃)₂), 1.22–1.12 (m, 8H, 3'-H, 4'-H, 5'-H, 6'-H), 0.83 ppm (t, J = 6.7 Hz, 3H, 7'-H). ¹³C NMR (75 MHz, CDCl₃) δ : 153.8 (9-C), 153.2 (5a-C), 152.9 (7-C), 142.5 (9b-C),

123.8 (3-C), 120.0 (3a-C), 106.6 (6-C), 106.4 (8-C), 101.1 (9a-C), 76.6 (OC(CH₃)₂), 59.3 (OCH₂CH₂CH₂OH), 48.8 (OCH₂CH₂CH₂OH), 44.5 (2'-C), 38.0 (C(CH₃)₂), 32.7 (OCH₂CH₂CH₂OH), 31.8, 30.0, 24.6, 22.6 (3'-C, 4'-C, 5'-C, 6'-C), 29.7 (C(CH₃)₂), 28.9 (OC-(CH₃)₂), 14.1 ppm (7'-C). HPLC-MS: [A, 80% → 95%]. t_R : 3.85 min (97%). MS (ES⁺, m/z) 401 [M + H]⁺. Anal. Calcd for C₂₄H₃₆N₂O₃: C 71.96, H 9.06; found, C 72.23, H, 9.10.

7-(1,1-Dimethylheptyl)-2,4-dihydro-9-(3-hydroxypropoxy)-2,4,4-

trimethylchromenof[4,3-c]pyrazole (29): The title compound was prepared from **6b** and 3-bromo-1-propanol. Column chromatography on silica gel (hexane/EtOAc, 1:1) afforded **29** as a pale orange oil (20 mg, 59%). ¹H NMR (300 MHz, CDCl₃) δ : 7.01 (s, 1H, 3-H), 6.52 (d, J = 1.6 Hz, 1H, 6-H), 6.45 (d, J = 1.6 Hz, 1H, 8-H), 4.18 (t, J = 6.5 Hz, 2H, OCH₂CH₂CH₂OH), 4.01 (s, 3H, NCH₃), 3.86–3.80 (m, 2H, OCH₂CH₂CH₂OH), 2.13–1.96 (m, 2H, OCH₂CH₂CH₂OH), 1.52 (s, 6H, OC(CH₃)₂), 1.42–1.38 (m, 2H, 2'-H), 1.19 (s, 6H, C(CH₃)₂), 1.16–0.92 (m, 8H, 3'-H, 4'-H, 5'-H, 6'-H), 0.77 ppm (t, J = 6.6 Hz, 3H, 7'-H). ¹³C NMR (75 MHz, CDCl₃) δ : 153.6 (9-C), 152.7 (5a-C), 150.8 (7-C), 139.5 (9b-C), 122.6 (3-C), 120.5 (3a-C), 109.2 (6-C), 107.6 (8-C), 101.3 (9a-C), 74.8 (OC(CH₃)₂), 59.5 (OCH₂CH₂CH₂OH), 50.1 (OCH₂CH₂CH₂OH), 45.3 (NCH₃), 39.5 (2'-C), 37.6 (C(CH₃)₂), 32.8 (OCH₂CH₂CH₂OH), 31.5, 30.9, 24.6, 22.6 (3'-C, 4'-C, 5'-C, 6'-C), 29.4 (C(CH₃)₂), 28.9 (OC(CH₃)₂), 13.0 ppm (7'-C). HPLC-MS: [A, 80% → 95%]. t_R : 4.07 min (93%). MS (ES⁺, m/z) 415 [M + H]⁺. Anal. Calcd for C₂₅H₃₈N₂O₂: C 72.43, H 9.24; found, C 72.12, H 8.98.

7-(1,1-Dimethylheptyl)-1-ethyl-1,4-dihydro-9-(3-hydroxypropoxy)-4,4-

dimethylchromenof[4,3-c]pyrazole (30): The title compound was prepared from **7a** and 3-bromo-1-propanol. Column chromatography on silica gel (hexane/EtOAc, 1:1) afforded **30** as a yellow solid (31 mg, 48%). mp: 91–93 °C. ¹H NMR (300 MHz, CDCl₃) δ : 7.37 (s, 1H, 3-H), 6.60 (d, J = 1.8 Hz, 1H, 6-H), 6.57 (d, J = 1.8 Hz, 1H, 8-H), 4.40–4.33 (m, 2H, OCH₂CH₂CH₂OH), 4.07–3.89 (m, 2H, NCH₂CH₃), 3.62–3.51 (m, 2H, OCH₂CH₂CH₂OH), 2.11 (p, J = 6.4 Hz, 2H, OCH₂CH₂CH₂OH), 1.55 (s, 6H, OC(CH₃)₂), 1.50 (t, J = 7.0 Hz, 3H, NCH₂CH₃), 1.41–1.36 (m, 2H, 2'-H), 1.24 (s, 6H, C(CH₃)₂), 1.12–0.98 (m, 8H, 3'-H, 4'-H, 5'-H, 6'-H), 0.85 ppm (t, J = 6.6 Hz, 3H, 7'-H). ¹³C NMR (75 MHz, CDCl₃) δ : 154.8 (9-C), 153.5 (5a-C), 151.6 (7-C), 141.4 (9b-C), 131.6 (3-C), 124.5 (3a-C), 110.3 (6-C), 107.9 (8-C), 102.6 (9a-C), 75.0 (OC(CH₃)₂), 63.2 (OCH₂CH₂CH₂OH), 57.6 (OCH₂CH₂CH₂OH), 46.5 (NCH₂CH₃), 44.7 (2'-C), 38.0 (C(CH₃)₂), 32.6 (OCH₂CH₂CH₂OH), 30.9, 29.6, 24.5, 21.7 (3'-C, 4'-C, 5'-C, 6'-C), 29.2 (C(CH₃)₂), 28.1 (OC(CH₃)₂), 15.0 (NCH₂CH₃), 14.1 ppm (7'-C). HPLC-MS: [A, 80% → 95%]. t_R : 3.42 min (99%). MS (ES⁺, m/z) 429 [M + H]⁺. Anal. Calcd for C₂₆H₄₀N₂O₃: C 72.86, H 9.41; found, C 72.75, H 9.63.

7-(1,1-Dimethylheptyl)-2-ethyl-2,4-dihydro-9-(3-hydroxypropoxy)-4,4-

dimethylchromeno-[4,3-c]pyrazole (31): The title compound was prepared from **7b** and 3-bromo-1-propanol. Column chromatography on silica gel (hexane/EtOAc, 1:1) afforded **31** as a yellow gummy solid (22 mg, 76%). ¹H NMR (300 MHz, CDCl₃) δ : 7.13 (s, 1H, 3-H), 6.58 (d, J = 1.6 Hz, 1H, 6-H), 6.52 (d, J = 1.6 Hz, 1H, 8-H), 4.31–4.25 (m, 2H,

$\text{OCH}_2\text{CH}_2\text{CH}_2\text{OH}$), 4.09–3.98 (m, 2H, NCH_2CH_3), 3.66–3.45 (m, 2H, $\text{OCH}_2\text{CH}_2\text{CH}_2\text{OH}$), 2.14–2.10 (m, 2H, $\text{OCH}_2\text{CH}_2\text{CH}_2\text{OH}$), 1.59 (s, 6H, $\text{OC}(\text{CH}_3)_2$), 1.51 (t, $J = 7.2$ Hz, 3H, NCH_2CH_3), 1.46–1.42 (m, 2H, 2'-H), 1.26 (s, 6H, $\text{C}(\text{CH}_3)_2$), 1.22–0.96 (m, 8H, 3'-H, 4'-H, 5'-H, 6'-H), 0.87–0.79 ppm (m, 3H, 7'-H). ^{13}C NMR (75 MHz, CDCl_3) δ : 153.5 (9-C), 152.8 (5a-C), 150.9 (7-C), 139.2 (9b-C), 120.8 (3-C), 120.3 (3a-C), 109.0 (6-C), 107.6 (8-C), 101.3 (9a-C), 74.8 ($\text{OC}(\text{CH}_3)_2$), 65.3 ($\text{OCH}_2\text{CH}_2\text{CH}_2\text{OH}$), 60.8 ($\text{OCH}_2\text{CH}_2\text{CH}_2\text{OH}$), 46.0 (NCH_2CH_3), 43.5 (2'-C), 37.1 ($\text{C}(\text{CH}_3)_2$), 31.5 ($\text{OCH}_2\text{CH}_2\text{CH}_2\text{OH}$), 30.7, 28.9, 23.6, 21.6 (3'-C, 4'-C, 5'-C, 6'-C), 28.1 ($\text{C}(\text{CH}_3)_2$), 27.8 ($\text{OC}(\text{CH}_3)_2$), 14.7 (NCH_2CH_3), 13.0 ppm (7'-C). HPLC-MS: [A, 80% \rightarrow 95%]. t_{R} : 4.63 min (96%). MS (ES^+ , m/z) 429 [$\text{M} + \text{H}$] $^+$. Anal. Calcd for $\text{C}_{26}\text{H}_{40}\text{N}_2\text{O}_3$: C 72.86, H 9.41; found, C 72.88, H 9.19.

1-(3,4-Dichlorophenyl)-7-(1,1-dimethylheptyl)-1,4-dihydro-9-(3-hydroxypropoxy)-4,4-dime-thylchromeno[4,3-c]pyrazole (32): The title compound was prepared from **8** and 3-bromo-1-propanol. Column chromatography on silica gel (hexane/EtOAc, 1:1) afforded **32** as a yellow oil (9 mg, 40%).

^1H NMR (300 MHz, CDCl_3) δ : 7.97 (d, $J = 2.5$ Hz, 1H, 2- H_{Ph}), 7.71 (dd, $J = 7.8, 2.5$ Hz, 1H, 6- H_{Ph}), 7.49 (d, $J = 7.8$ Hz, 1H, 5- H_{Ph}), 7.47 (s, 1H, 3-H), 6.62 (d, $J = 1.7$ Hz, 1H, 6-H), 6.60 (d, $J = 1.7$ Hz, 1H, 8-H), 4.12 (t, $J = 6.2$ Hz, 2H, $\text{OCH}_2\text{CH}_2\text{CH}_2\text{OH}$), 3.88 (t, $J = 6.2$ Hz, 2H, $\text{OCH}_2\text{CH}_2\text{CH}_2\text{OH}$), 2.09 (p, $J = 6.2$ Hz, 2H, $\text{OCH}_2\text{CH}_2\text{CH}_2\text{OH}$), 1.65 (s, 6H, $\text{OC}(\text{CH}_3)_2$), 1.60–1.40 (m, 2H, 2'-H), 1.22 (s, 6H, $\text{C}(\text{CH}_3)_2$), 1.20–0.94 (m, 8H, 3'-H, 4'-H, 5'-H, 6'-H), 0.83–0.72 ppm (m, 3H, 7'-H). ^{13}C NMR (75 MHz, CDCl_3) δ : 155.2 (9-C), 153.9 (5a-C), 152.5 (7-C), 140.7 (1- C_{Ph}), 139.7 (9b-C), 136.0 (3- C_{Ph}), 130.3 (3-C), 129.6 (4- C_{Ph}), 127.4 (5- C_{Ph}), 125.3 (2- C_{Ph}), 124.1 (6- C_{Ph}), 121.6 (3a-C), 110.7 (6-C), 108.5 (8-C), 102.3 (9a-C), 75.1 ($\text{OC}(\text{CH}_3)_2$), 67.9 ($\text{OCH}_2\text{CH}_2\text{CH}_2\text{OH}$), 62.1 ($\text{OCH}_2\text{CH}_2\text{CH}_2\text{OH}$), 44.6 (2'-C), 38.2 ($\text{C}(\text{CH}_3)_2$), 31.7 ($\text{OCH}_2\text{CH}_2\text{CH}_2\text{OH}$), 30.9, 29.1, 24.0, 21.3 (3'-C, 4'-C, 5'-C, 6'-C), 28.6 ($\text{C}(\text{CH}_3)_2$), 27.9 ($\text{OC}(\text{CH}_3)_2$), 14.3 ppm (7'-C). HPLC-MS: [A, 80% \rightarrow 95%]. t_{R} : 4.58 min (93%). MS (ES^+ , m/z) 545 [$\text{M} + \text{H}$] $^+$. Anal. Calcd for $\text{C}_{30}\text{H}_{38}\text{Cl}_2\text{N}_2\text{O}_3$: C 66.05, H 7.02; found, C 65.81, H 7.13.

1-(2,4-Dichlorophenyl)-7-(1,1-dimethylheptyl)-1,4-dihydro-9-(3-hydroxypropoxy)-4,4-dime-thyl-9-methoxychromeno[4,3-c]pyrazole (33): The title compound was prepared from **9** and 3-bromo-1-propanol. Column chromatography on silica gel (hexane/EtOAc, 1:1) afforded **33** as a yellow gummy solid (18 mg, 31%).

^1H NMR (300 MHz, CDCl_3) δ : 7.57 (s, 1H, 3-H), 7.51 (d, $J = 1.8$ Hz, 1H, 3- H_{Ph}), 7.25–7.018 (m, 2H, 5- H_{Ph} , 6- H_{Ph}), 6.66 (d, $J = 1.6$ Hz, 1H, 6-H), 6.40 (d, $J = 1.6$ Hz, 1H, 8-H), 3.82–3.60 (m, 2H, $\text{OCH}_2\text{CH}_2\text{CH}_2\text{OH}$), 3.56 (t, $J = 6.0$ Hz, 2H, $\text{OCH}_2\text{CH}_2\text{CH}_2\text{OH}$), 1.90–1.85 (m, 2H, $\text{OCH}_2\text{CH}_2\text{CH}_2\text{OH}$), 1.63 (s, 6H, $\text{OC}(\text{CH}_3)_2$), 1.57–1.46 (m, 2H, 2'-H), 1.24 (s, 6H, $\text{C}(\text{CH}_3)_2$), 1.22–0.96 (m, 8H, 3'-H, 4'-H, 5'-H, 6'-H), 0.84 ppm (t, $J = 6.6$ Hz, 3H, 7'-H). ^{13}C NMR (75 MHz, CDCl_3) δ : 153.6 (9-C), 153.3 (5a-C), 153.2 (7-C), 140.0 (1- C_{Ph}), 134.8 (9b-C), 134.4 (2- C_{Ph}), 133.5 (4- C_{Ph}), 131.1 (3-C), 129.6 (3- C_{Ph}), 128.6 (5- C_{Ph}), 127.0 (6- C_{Ph}), 123.5 (3a-C), 109.1 (6-C), 103.7 (8-C), 103.0 (9a-C), 76.5 ($\text{OC}(\text{CH}_3)_2$), 64.9 ($\text{OCH}_2\text{CH}_2\text{CH}_2\text{OH}$), 59.4 ($\text{OCH}_2\text{CH}_2\text{CH}_2\text{OH}$), 44.3 (2'-C), 38.1 ($\text{C}(\text{CH}_3)_2$), 31.6 ($\text{OCH}_2\text{CH}_2\text{CH}_2\text{OH}$), 31.0, 29.8, 24.5, 22.5 (3'-C, 4'-C, 5'-C, 6'-C), 28.5 ($\text{C}(\text{CH}_3)_2$), 27.3 ($\text{C}(\text{CH}_3)_2$), 14.0 ppm (7'-C). HPLC-MS: [A, 80% \rightarrow 95%]. t_{R} : 4.72 min (96%). MS (ES^+ , m/z) 545 [$\text{M} + \text{H}$] $^+$. Anal. Calcd for $\text{C}_{30}\text{H}_{38}\text{Cl}_2\text{N}_2\text{O}_3$: C 66.05, H 7.02; found, C 66.26, H 6.97.

7-(1,1-Dimethylheptyl)-2,4-dihydro-9-(2-hydroxyethoxy)-4,4-dimethylchromeno[4,3-c]pyra-zole (34): The title compound was prepared from **5** and 2-bromoethanol. Column chromatography on silica gel (hexane/EtOAc, 1:1) afforded the title compound as a white solid (12 mg, 54%). mp: 85–87 °C. ¹H NMR (300 MHz, CDCl₃) δ: 7.34 (s, 1H, 3-H), 6.60 (d, *J* = 1.7 Hz, 1H, 6-H), 6.52 (d, *J* = 1.7 Hz, 1H, 8-H), 4.19–4.07 (m, 2H, OCH₂CH₂OH), 3.56–3.45 (m, 2H, OCH₂CH₂OH), 1.64 (s, 6H, OC(CH₃)₂), 1.60–1.48 (m, 2H, 2'-H), 1.25 (s, 6H, C(CH₃)₂), 1.23–0.97 (m, 8H, 3'-H, 4'-H, 5'-H, 6'-H), 0.88–0.79 ppm (m, 3H, 7'-H). ¹³C NMR (75 MHz, CDCl₃) δ: 155.2 (9-C), 154.1 (5a-C), 152.6 (7-C), 141.3 (9b-C), 124.9 (3-C), 121.9 (3a-C), 109.3 (6-C), 106.6 (8-C), 102.7 (9a-C), 74.8 (OC(CH₃)₂), 60.1 (OCH₂CH₂OH), 51.4 (OCH₂CH₂OH), 43.2 (2'-C), 37.7 (C(CH₃)₂), 32.0, 31.4, 25.7, 22.3 (3'-C, 4'-C, 5'-C, 6'-C), 29.8 (C(CH₃)₂), 27.9 (OC(CH₃)₂), 15.0 ppm (7'-C). HPLC-MS: [A, 80% → 95%]. *t*_R: 3.45 min (93%). MS (ES⁺, *m/z*) 387 [M + H]⁺. Anal. Calcd for C₂₃H₃₄N₂O₃: C 71.47, H 8.87; found, C 71.80, H, 8.64.

7-(1,1-Dimethylheptyl)-2,4-dihydro-9-(2-hydroxyethoxy)-2,4,4-trimethylchromeno[4,3-c]py-razole (35): The title compound was prepared from **6b** and 2-bromoethanol. Column chromatography on silica gel (hexane/EtOAc, 1:2) afforded **35** as a pale yellow oil (16 mg, 73%). ¹H NMR (300 MHz, CDCl₃) δ: 7.19 (s, 1H, 3-H), 6.59 (d, *J* = 1.8 Hz, 1H, 6-H), 6.51 (d, *J* = 1.8 Hz, 1H, 8-H), 4.30–4.25 (m, 2H, OCH₂CH₂OH), 4.05 (s, 3H, NCH₃), 3.81–3.74 (m, 2H, OCH₂CH₂OH), 1.60 (s, 6H, OC(CH₃)₂), 1.40–1.35 (m, 2H, 2'-H), 1.21 (s, 6H, C(CH₃)₂), 1.12–0.89 (m, 8H, 3'-H, 4'-H, 5'-H, 6'-H), 0.81 ppm (t, *J* = 6.9 Hz, 3H, 7'-H). ¹³C NMR (75 MHz, CDCl₃) δ: 154.1 (9-C), 153.5 (5a-C), 152.3 (7-C), 140.5 (9b-C), 123.8 (3-C), 121.4 (3a-C), 111.2 (6-C), 108.5 (8-C), 103.6 (9a-C), 76.0 (OC(CH₃)₂), 64.3 (OCH₂CH₂OH), 59.2 (OCH₂CH₂OH), 40.6 (NCH₃), 39.0 (2'-C), 38.1 (C(CH₃)₂), 32.1, 30.8, 25.7, 21.3 (3'-C, 4'-C, 5'-C, 6'-C), 29.7 (C(CH₃)₂), 28.0 (OC(CH₃)₂), 14.7 ppm (7'-C). HPLC-MS: [A, 80% → 95%]. *t*_R: 3.41 min (99%). MS (ES⁺, *m/z*) 401 [M + H]⁺. Anal. Calcd for C₂₄H₃₆N₂O₃: C 71.96, H 9.06; found, C 71.67, H, 8.84.

7-(1,1-Dimethylheptyl)-2-ethyl-2,4-dihydro-9-(2-hydroxyethoxy)-4,4-dimethylchromeno[4,3-c]pyrazole (36): The title compound was prepared from **7b** and 2-bromoethanol. Column chromatography on silica gel (hexane/EtOAc, 1:1) afforded **36** as a white oil (13 mg, 48%). ¹H NMR (300 MHz, CDCl₃) δ: 7.22 (s, 1H, 3-H), 6.61 (d, *J* = 1.8 Hz, 1H, 6-H), 6.57 (d, *J* = 1.8 Hz, 1H, 8-H), 4.30–4.23 (m, 2H, OCH₂CH₂OH), 3.95 (q, *J* = 7.1 Hz, 2H, NCH₂CH₃), 3.63–3.59 (m, 2H, OCH₂CH₂OH), 1.62 (s, 6H, OC(CH₃)₂), 1.54 (t, *J* = 7.1 Hz, 3H, NCH₂CH₃), 1.40–1.33 (br s, 2H, 2'-H), 1.28 (s, 6H, C(CH₃)₂), 1.23–0.91 (m, 8H, 3'-H, 4'-H, 5'-H, 6'-H), 0.88–0.81 ppm (m, 3H, 7'-H). ¹³C NMR (75 MHz, CDCl₃) δ: 155.2 (9-C), 153.7 (5a-C), 151.8 (7-C), 140.3 (9b-C), 124.6 (3-C), 121.5 (3a-C), 110.2 (6-C), 108.6 (8-C), 102.4 (9a-C), 75.1 (OC(CH₃)₂), 68.5 (OCH₂CH₂OH), 61.3 (OCH₂CH₂OH), 47.3 (NCH₂CH₃), 42.9 (2'-C), 37.7 (C(CH₃)₂), 31.7, 30.2, 25.3, 22.5 (3'-C, 4'-C, 5'-C, 6'-C), 29.2 (C(CH₃)₂), 28.3 (OC(CH₃)₂), 15.2 (NCH₂CH₃), 14.3 ppm (7'-C). HPLC-MS: [A, 80% → 95%]. *t*_R: 5.22 min (92%). MS (ES⁺, *m/z*) 415 [M + H]⁺. Anal. Calcd for C₂₅H₃₈N₂O₃: C 72.43, H 9.24; found, C 72.60, H 9.08.

9-(3-Bromopropoxy)-7-(1,1-dimethylheptyl)-2,4-dihydro-2,4,4-trimethylchromeno[4,3-c]py-razole (37): The title compound was prepared from **6b** and 1,3-dibromopropane.

Column chromatography on silica gel (hexane/EtOAc, 3:1) afforded **37** as a white solid (27 mg, 47%). mp: 96–98 °C. ¹H NMR (300 MHz, CDCl₃) δ: 7.49 (s, 1H, 3-H), 6.73 (d, *J* = 1.8 Hz, 1H, 6-H), 6.68 (d, *J* = 1.8 Hz, 1H, 8-H), 4.34 (t, *J* = 6.3 Hz, 2H, OCH₂CH₂CH₂Br), 4.07 (s, 3H, NCH₃), 3.87 (t, *J* = 6.3 Hz, 2H, OCH₂CH₂CH₂Br), 2.49 (p, *J* = 6.3 Hz, 2H, OCH₂CH₂CH₂Br), 1.60 (s, 6H, OC(CH₃)₂), 1.58–1.46 (m, 2H, 2'-H), 1.27 (s, 6H, C(CH₃)₂), 1.24–0.94 (m, 8H, 3'-H, 4'-H, 5'-H, 6'-H), 0.90–0.77 ppm (m, 3H, 7'-H). ¹³C NMR (75 MHz, CDCl₃) δ: 153.0 (9-C), 152.5 (5a-C), 151.3 (7-C), 141.0 (9b-C), 124.7 (3-C), 121.8 (3a-C), 109.9 (6-C), 108.5 (8-C), 103.2 (9a-C), 75.1 (OC(CH₃)₂), 62.3 (OCH₂CH₂CH₂Br), 46.7 (NCH₃), 38.6 (2'-C), 37.3 (C(CH₃)₂), 33.1 (OCH₂CH₂CH₂Br), 31.7 (OCH₂CH₂CH₂Br), 30.8, 30.1, 25.6, 21.3 (3'-C, 4'-C, 5'-C, 6'-C), 29.7 (C(CH₃)₂), 28.1 (OC(CH₃)₂), 14.0 ppm (7'-C). HPLC-MS: [A, 80% → 95%]. *t*_R: 5.55 min (96%). MS (ES⁺, *m/z*) 477 [M + H]⁺. Anal. Calcd for C₂₅H₃₇BrN₂O₂: C 62.89, H 7.81; found, C 63.05, H 7.72.

9-(3-Bromopropoxy)-7-(1,1-dimethylheptyl)-2-ethyl-2,4-dihydro-4,4-

dimethylchromeno[4,3-c]pyrazole (38): The title compound was prepared from **7b** and 1,3-dibromopropane. Column chromatography on silica gel (hexane/EtOAc, 3:1) afforded **38** as a yellow oil (15 mg, 55%). ¹H NMR (300 MHz, CDCl₃) δ: 7.21 (s, 1H, 3-H), 6.62 (d, *J* = 1.7 Hz, 1H, 6-H), 6.56 (d, *J* = 1.7 Hz, 1H, 8-H), 4.29–4.16 (m, 2H, OCH₂CH₂CH₂Br), 4.11 (q, 2H, *J* = 7.0 Hz, NCH₂CH₃), 3.52–3.47 (m, 2H, OCH₂CH₂CH₂Br), 2.12–2.04 (m, 2H, OCH₂CH₂CH₂Br), 1.65 (s, 6H, OC(CH₃)₂), 1.60 (t, *J* = 7.0 Hz, 3H, NCH₂CH₃), 1.40–1.34 (m, 2H, 2'-H), 1.29 (s, 6H, C(CH₃)₂), 1.23–0.98 (m, 8H, 3'-H, 4'-H, 5'-H, 6'-H), 0.86 ppm (t, *J* = 7.1 Hz, 3H, 7'-H). ¹³C NMR (75 MHz, CDCl₃) δ: 152.9 (9-C), 152.1 (5a-C), 150.3 (7-C), 138.4 (9b-C), 121.7 (3-C), 120.1 (3a-C), 108.3 (6-C), 106.5 (8-C), 101.8 (9a-C), 75.3 (OC(CH₃)₂), 65.2 (OCH₂CH₂CH₂Br), 45.9 (NCH₂CH₃), 44.1 (2'-C), 38.0 (C(CH₃)₂), 32.7 (OCH₂CH₂CH₂Br), 31.9 (OCH₂CH₂CH₂Br), 31.0, 29.8, 24.2, 21.6 (3'-C, 4'-C, 5'-C, 6'-C), 28.7 (C(CH₃)₂), 27.5 (OC(CH₃)₂), 14.8 (NCH₂CH₃), 13.5 ppm (7'-C). HPLC-MS: [A, 80% → 95%]. *t*_R: 5.14 min (95%). MS (ES⁺, *m/z*) 491 [M + H]⁺. Anal. Calcd for C₂₆H₃₉BrN₂O₂: C 63.54, H 8.00; found, C 63.87, H 8.12.

9-(2-Bromoethoxy)-7-(1,1-dimethylheptyl)-1-ethyl-1,4-dihydro-4,4-

dimethylchromeno[4,3-c]pyrazole (39): The title compound was prepared from **7a** and 1,2-dibromoethane. Column chromatography on silica gel (hexane/EtOAc, 2:1) afforded **39** as a yellow oil (16 mg, 64%). ¹H NMR (300 MHz, CDCl₃) δ: 7.29 (s, 1H, 3-H), 6.69 (d, *J* = 1.5 Hz, 1H, 6-H), 6.61 (d, *J* = 1.5 Hz, 1H, 8-H), 4.38–4.31 (m, 2H, OCH₂CH₂Br), 4.03 (q, *J* = 7.5 Hz, 2H, NCH₂CH₃), 3.71–3.62 (m, 2H, OCH₂CH₂Br), 1.56 (s, 6H, OC(CH₃)₂), 1.53 (t, *J* = 7.5 Hz, 3H, NCH₂CH₃), 1.50–1.42 (m, 2H, 2'-H), 1.27 (s, 6H, C(CH₃)₂), 1.17–1.04 (m, 8H, 3'-H, 4'-H, 5'-H, 6'-H), 0.88 ppm (t, *J* = 6.6 Hz, 3H, 7'-H). ¹³C NMR (75 MHz, CDCl₃) δ: 155.3 (9-C), 154.0 (5a-C), 152.5 (7-C), 142.6 (9b-C), 133.7 (3-C), 124.8 (3a-C), 109.9 (6-C), 108.1 (8-C), 103.5 (9a-C), 76.2 (OC(CH₃)₂), 64.7 (OCH₂CH₂Br), 45.9 (NCH₂CH₃), 43.8 (2'-C), 37.5 (C(CH₃)₂), 31.2 (OCH₂CH₂Br), 30.3, 29.7, 25.7, 22.3 (3'-C, 4'-C, 5'-C, 6'-C), 29.0 (C(CH₃)₂), 27.7 (OC(CH₃)₂), 15.2 (NCH₂CH₃), 14.0 ppm (7'-C). HPLC-MS: [A, 80% → 95%]. *t*_R: 5.64 min (95%). MS (ES⁺, *m/z*) 477 [M + H]⁺. Anal. Calcd for C₂₅H₃₇BrN₂O₂: C 62.89, H 7.81; found, C 62.61, H 8.03.

7-(1,1-Dimethylheptyl)-1-ethyl-1,4,9,10-tetrahydro-4,4-dimethyl-8H-pyrano[2',3':5,6]chrome-no[4,3-c]pyrazole (40): Compound **30** (25 mg, 0.06 mmol) in 1.5 mL of dry toluene was added to a stirred suspension of P₂O₅ (16 mg, 0.12 mmol) in 2 mL of dry toluene under nitrogen atmosphere, and the mixture was refluxed for 1 h. After completion, the reaction mixture was cooled to room temperature and filtered. The filtrate was diluted with EtOAc and washed with NaOH (0.1 N), water, and brine and extracted three times with EtOAc. The combined organic layers were dried over MgSO₄, and the solvent was removed under vacuum. Column chromatography on silica gel (hexane/EtOAc, 4:1) afforded **40** as a yellow oil (20 mg, 87%). ¹H NMR (300 MHz, CDCl₃) δ: 7.39 (s, 1H, 3-H), 6.59 (s, 1H, 6-H), 4.41–4.32 (m, 2H, OCH₂CH₂CH₂), 4.21–4.16 (m, 2H, NCH₂CH₃), 2.84–2.78 (m, 2H, OCH₂CH₂CH₂), 2.09–2.01 (m, 2H, OCH₂CH₂CH₂), 1.61 (s, 6H, OC(CH₃)₂), 1.56 (t, *J* = 6.7 Hz, 3H, NCH₂CH₃), 1.45–1.40 (m, 2H, 2'-H), 1.27 (s, 6H, C(CH₃)₂), 1.10–0.96 (m, 8H, 3'-H, 4'-H, 5'-H, 6'-H), 0.85–0.79 ppm (m, 3H, 7'-H). ¹³C NMR (75 MHz, CDCl₃) δ: 153.9 (11a-C), 152.8 (5a-C), 152.0 (7-C), 142.5 (11c-C), 132.3 (3-C), 128.0 (3a-C), 109.6 (7a-C), 108.3 (6-C), 103.5 (11b-C), 74.9 (OC(CH₃)₂), 63.7 (OCH₂CH₂CH₂), 46.1 (NCH₂CH₃), 43.4 (2'-C), 37.7 (C(CH₃)₂), 32.0, 31.3, 29.4, 24.6, 23.9, 21.2 (3'-C, 4'-C, 5'-C, 6'-C, OCH₂CH₂CH₂), 29.0 (C(CH₃)₂), 28.5 (OC(CH₃)₂), 15.4 (NCH₂CH₃), 14.1 ppm (7'-C). HPLC-MS: [A, 80% → 95%]. *t*_R: 5.82 min (95%). MS (ES⁺, *m/z*) 411 [M + H]⁺. Anal. Calcd for C₂₆H₃₈N₂O₂: C 76.06, H 9.33; found, C 75.82, H 9.08.

7-(1,1-Dimethylheptyl)-2-ethyl-2,4,9,10-tetrahydro-4,4-dimethyl-8H-pyrano[2',3':5,6]chrome-no[4,3-c]pyrazole (41): The title compound was prepared from **31** (71 mg, 0.16 mmol) and P₂O₅ (46 mg, 0.33 mmol) following the procedure previously described for **40**. Column chromatography on silica gel (hexane/EtOAc, 4:1) afforded **41** as a pale yellow oil (23 mg, 52%). ¹H NMR (300 MHz, CDCl₃) δ: 7.20 (s, 1H, 3-H), 6.61 (s, 1H, 6-H), 4.31–4.27 (m, 2H, OCH₂CH₂CH₂), 4.20–4.16 (m, 2H, NCH₂CH₃), 2.72–2.69 (m, 2H, OCH₂CH₂CH₂), 2.11–2.04 (m, 2H, OCH₂CH₂CH₂), 1.67 (s, 6H, OC(CH₃)₂), 1.52 (t, *J* = 7.0 Hz, 3H, NCH₂CH₃), 1.50–1.46 (m, 2H, 2'-H), 1.26 (s, 6H, C(CH₃)₂), 1.15–0.99 (m, 8H, 3'-H, 4'-H, 5'-H, 6'-H), 0.84 ppm (t, *J* = 6.9 Hz, 3H, 7'-H). ¹³C NMR (75 MHz, CDCl₃) δ: 154.0 (11a-C), 153.7 (5a-C), 152.5 (7-C), 140.9 (11c-C), 122.3 (3-C), 119.6 (3a-C), 108.8 (7a-C), 108.1 (6-C), 104.2 (11b-C), 75.3 (OC(CH₃)₂), 65.0 (OCH₂CH₂CH₂), 45.9 (NCH₂CH₃), 44.1 (2'-C), 38.2 (C(CH₃)₂), 31.4, 30.8, 29.5, 24.9, 24.0, 22.6 (3'-C, 4'-C, 5'-C, 6'-C, OCH₂CH₂CH₂), 29.1 (C(CH₃)₂), 28.7 (OC(CH₃)₂), 14.9 (NCH₂CH₃), 13.8 ppm (7'-C). HPLC-MS: [A, 80% → 95%]. *t*_R: 5.07 min (98%). MS (ES⁺, *m/z*) 411 [M + H]⁺. Anal. Calcd for C₂₆H₃₈N₂O₂: C 76.06, H 9.33; found, C 76.35, H 8.99.

7-(1,1-Dimethylheptyl)-4,4-dimethyl-4H-chromeno[3,4-d]-isoxazol-9-ol (42): A solution of **4**³⁴ (0.12 g, 0.35 mmol) and hydroxylamine hydrochloride (49 mg, 0.71 mmol) in ethanol (4 mL) was refluxed for 45 min. After cooling the mixture, the crude was filtered and washed with cold ethanol. After removal of the solvent, the crude was purified by chromatography on silica gel (hexane/EtOAc, 2:1) to obtain **42** as a pale yellow solid (0.11 g; 91%). mp: 109–111 °C. ¹H NMR (300 MHz, CDCl₃) δ: 8.12 (s, 1H, 3-H), 6.57 (d, *J* = 1.6 Hz, 1H, 8-H), 6.55 (d, *J* = 1.4 Hz, 6-H), 1.64 (s, 6H, OC(CH₃)₂), 1.59–1.47 (m, 2H, 2'-H), 1.24 (s, 6H, C(CH₃)₂), 1.17–1.09 (br s, 8H, 3'-H, 4'-H, 5'-H, 6'-H), 0.82 ppm (t, *J* = 7.0 Hz, 3H, 7'-H). ¹³C NMR (75 MHz, CDCl₃) δ: 160.2 (9-C), 156.6 (9b-C), 153.6 (5a-C),

151.7 (7-C), 145.4 (3-C), 119.4 (9a-C), 109.5 (8-C), 108.1 (6-C), 105.9 (3a-C), 78.0 (OC(CH₃)₂), 44.5 (2'-C), 38.5 (C(CH₃)₂), 31.9, 30.1, 24.8 (3'-C, 4'-C, 5'-C), 29.2 (C(CH₃)₂), 28.9 (OC(CH₃)₂), 22.9 (6'-C), 14.3 ppm (7'-C). HPLC-MS: [A, 80% → 95%]. t_R : 2.77 min (99%). MS (ES⁺, m/z) 344 [M + H]⁺. Anal. Calcd for C₂₁H₂₉NO₃ 73.44, H 8.51; found, C 73.81, H, 8.59.

7-(1,1-Dimethylheptyl)-9-methoxy-4,4-dimethyl-4H-chromeno-[3,4-d]isoxazole

(43): The title compound was prepared from **42** (30 mg, 0.09 mmol), sodium hydride (3 mg, 0.13 mmol), and iodomethane (16 μ L, 0.26 mmol) following the procedure described for **15**. Column chromatography on silica gel (hexane/EtOAc, 2:1) afforded **43** as a yellow oil (19 mg, 61%). ¹H NMR (300 MHz, CDCl₃) δ : 8.10 (s, 1H, 3-H), 6.47 (d, J = 1.6 Hz, 1H, 8-H), 6.35 (d, J = 1.6 Hz, 1H, 6-H), 3.59 (s, 3H, OCH₃), 1.77 (s, 6H, OC(CH₃)₂), 1.54–1.31 (m, 2H, 2'-H), 1.26 (s, 6H, C(CH₃)₂), 1.17–0.98 (m, 8H, 3'-H, 4'-H, 5'-H, 6'-H), 0.83–0.78 ppm (m, 3H, 7'-H). ¹³C NMR (75 MHz, CDCl₃) δ : 165.6 (9-C), 162.2 (9b-C), 157.8 (5a-C), 153.5 (7-C), 150.1 (3-C), 118.0 (9a-C), 108.3 (8-C), 106.5 (6-C), 103.0 (3a-C), 76.7 (OC(CH₃)₂), 52.2 (OCH₃), 44.3 (2'-C), 39.4 (C(CH₃)₂), 32.1, 30.3, 24.8, 23.6 (3'-C, 4'-C, 5'-C, 6'-C), 28.7 (C(CH₃)₂), 26.0 (OC(CH₃)₂), 14.6 ppm (7'-C). HPLC-MS: [A, 80% → 95%]. t_R : 4.97 min (98%). MS (ES⁺, m/z) 358 [M + H]⁺. Anal. Calcd for C₂₂H₃₁NO₃: C 73.92, H 8.74; found, C 74.11, H, 8.95.

7-(1,1-Dimethylheptyl)-9-(3-hydroxypropoxy)-4,4-dimethyl-4H-chromeno[3,4-d]isoxazole (44):

The title compound was prepared from **42** (50 mg, 0.14 mmol), sodium hydride (7 mg, 0.29 mmol), and 3-bromo-1-propanol (99 μ L, 0.72 mmol) as described for compounds **22–39**. Column chromatography on silica gel (hexane/EtOAc, 2:1) afforded **44** as a yellow oil (13 mg, 22%). ¹H NMR (300 MHz, CDCl₃) δ : 8.11 (s, 1H, 3-H), 6.69 (d, J = 1.6 Hz, 1H, 8-H), 6.58 (d, J = 1.6 Hz, 1H, 6-H), 4.15 (t, J = 7.1 Hz, 2H, OCH₂CH₂CH₂OH), 3.78 (t, J = 4.7 Hz, 2H, OCH₂CH₂CH₂OH), 2.11–2.09 (m, 2H, OCH₂CH₂CH₂OH), 1.65 (s, 6H, OC(CH₃)₂), 1.61–1.57 (m 2H, 2'-H), 1.51 (s, 6H, C(CH₃)₂), 1.23–1.14 (m, 8H, 3'-H, 4'-H, 5'-H, 6'-H), 0.86–0.80 ppm (m, 3H, 7'-H). ¹³C NMR (75 MHz, CDCl₃) δ : 160.5 (9-C), 155.7 (9b-C), 154.0 (5a-C), 150.9 (7-C), 143.5 (3-C), 120.6 (9a-C), 108.9 (8-C), 106.3 (6-C), 105.8 (3a-C), 75.0 (OC(CH₃)₂), 66.3 (OCH₂CH₂CH₂OH), 62.8 (OCH₂CH₂CH₂OH), 44.3 (2'-C), 40.1 (OCH₂CH₂CH₂OH), 38.3 (C(CH₃)₂), 32.7, 31.5, 23.9, 22.6 (3'-C, 4'-C, 5'-C, 6'-C), 28.3 (C(CH₃)₂), 27.1 (OC(CH₃)₂), 14.7 ppm (7'-C). HPLC-MS: [A, 80% → 95%]. t_R : 2.96 min (95%). MS (ES⁺, m/z) 402 [M + H]⁺. Anal. Calcd for C₂₄H₃₅NO₄: C 71.79, H 8.79; found, C 72.06, H, 8.55.

Pharmacological Assays

Radioligand Binding Experiments—Commercial membranes purified from cells transfected with human CB₁ or CB₂ receptors (RBHCB1M400UA and RBXCB2M400UA) were supplied by PerkinElmer Life and Analytical Sciences (Boston, MA, USA). The protein concentration was 8 μ g/well for CB₁ and 4 μ g/well for the CB₂ receptor. The binding buffer was 50 mM TrisCl, 5 mM MgCl₂, 2.5 mM EDTA, and 0.5 mg/mL BSA (pH 7.4) for CB₁, and 50 mM TrisCl, 5 mM MgCl₂, 2.5 mM EGTA, and 1 mg/mL BSA (pH 7.5) for CB₂. The radioligand [³H]-CP55940 (PerkinElmer, Boston, MA, USA) was used at a concentration of membrane KD \times 0.8 nM, and the final incubation volume was 200 μ L for

CB₁ and 600 μ L for CB₂ receptors. 96-well plates and the tubes necessary for the experiment were previously siliconized with Sigmacote (Sigma-Aldrich, Madrid, Spain). Membranes were resuspended in the corresponding buffer and were incubated (90 min at 30 °C) with the radioligand and each compound at a high concentration (40 μ M) with the purpose of determining the % of radioligand displacement. Only in those cases in which radioligand displacement was greater than 70%, a complete competition curve with different compound concentrations (10–11–10⁻⁴ M) was carried out to obtain the K_i values. Nonspecific binding was determined with 10 μ M WIN55212-2 (Sigma-Aldrich, Madrid, Spain) and total radioligand binding by incubation with the membranes in the absence of any compound. Filtration was performed by a Harvester filtermate (PerkinElmer, Boston, MA, USA) with Filtermat A GF/C filters pretreated with polyethylenimine 0.05%. After filtering, the filter was washed nine times with binding buffer and dried, and a melt-on scintillation sheet (MeltilexTM A, PerkinElmer, Boston, MA, USA) was melted onto it. Then, radioactivity was quantified by a liquid scintillation counter (Wallac MicroBeta Trilux, PerkinElmer, Boston, MA, USA). Competition binding data were analyzed by using GraphPad Prism, version 5.02 (GraphPad Software Inc., San Diego, CA, USA), and K_i values are expressed as the mean \pm SEM of at least three experiments performed in triplicate for each point.

cAMP Determination Assays—Determination of cAMP levels in HEK293 cells stably expressing the CB₂ receptor was performed using the Lance-Ultra cAMP kit (PerkinElmer) according to the manufacturer's instructions. Briefly, HEK293 cells expressing the CB₂ receptor were dispensed in white 384-well microplates at a density of 5,000 cells per well. Finally, cells were incubated for 60 min at room temperature with HTRF assay reagents, and fluorescence at 665 nm was analyzed on a PHERAstar Flagship microplate reader equipped with an HTRF optical module (BMG Labtech). Data analysis was made based on the fluorescence ratio emitted by the labeled cAMP probe (665 nm) over the light emitted by the europium cryptate-labeled anti-cAMP antibody (620 nm). A standard curve was used to calculate cAMP concentration. Forskolin stimulated cAMP levels were normalized to 100%. Data was analyzed by using the GraphPad Prism program using nonlinear regression analysis. EC₅₀ and E_{max} values are expressed as the mean \pm SEM of at least three experiments performed in triplicate.

[³⁵S]-GTP γ S Binding Assays

Protocol for CB₁ Receptors: Cell Culture—HEK293-CB₁R cells were grown to confluence under 5% CO₂ in Dulbecco's modified Eagle's medium (Lonza) containing 10% fetal bovine serum (Sigma-Aldrich), 1 \times penicillin–streptomycin–amphotericin B antibiotics (Lonza), and ultraglutamine 2 mM (Lonza). Membrane preparation: cells were washed twice with ice-cold phosphate-buffered saline, detached from flasks by incubation with lifting buffer (glucose 5.6 mM, KCl 5 mM, HEPES 5 mM, NaCl 137 mM, and EGTA 1 mM, pH 7.4), and collected by centrifugation (500g). The cells were resuspended in ice-cold lysis buffer (MgSO₄ 0.2 mM, KH₂PO₄ 0.38 mM, Na₂HPO₄ 0.61 mM, pH 7.4) and homogenized using a glass-PTFE homogenizer. Crude membranes were isolated by centrifugation for 20 min at 20,000g. The resulting membrane pellets were resuspended in 50 mM Tris-HCl buffer (pH 7.4) and stored at –80 °C in aliquots of 0.8 mg/mL protein determined for Bio-

Rad DC Protein Assay. All procedures were performed at 4 °C. Agonist-stimulated [³⁵S]GTP γ S binding: cannabinoid agonist stimulation of [³⁵S]GTP γ S binding was determined using several concentrations of compounds from 10⁻⁴ to 10⁻¹¹ M and incubated with HEK293-CB₁R membranes (20 μ g/well) for 60 min at 30 °C in assay buffer (100 mM NaCl, 50 mM Tris-HCl, 5 mM MgCl₂, 1 mM EGTA, 1 mM DTT, 50 μ M GDP, 10 mU/mL adenosine deaminase, and 1 mg/mL BSA, pH 7.4) containing 0.1 nM [³⁵S]GTP γ S (PerkinElmer). Nonspecific binding was determined in the presence of 10 μ M GTP γ S. 96-Well plates and the tubes necessary for the experiment were previously siliconized with Sigmacote (Sigma-Aldrich).

Experiments were terminated by rapid filtration performed by a Harvester filtermate (PerkinElmer) with Filtermat A GF/C filters. After filtering, the filter was washed nine times with filtration buffer (50 mM Tris-HCl and 1 mg/mL BSA, pH 7.4) and dried, and a melt-on scintillation sheet (Meltilex A, PerkinElmer) was melted onto it. Then, radioactivity was quantified by a liquid scintillation spectrophotometer (Wallac MicroBeta Trilux, PerkinElmer). Data were analyzed by nonlinear regression analysis of sigmoidal dose–response curves using GraphPad Prism 5.01 (GraphPad, San Diego, CA). EC₅₀ values are expressed as the mean \pm SEM of at least three experiments performed in triplicate for each point.

Protocol for CB₂ Receptors—[³⁵S]-GTP γ S binding analyses were carried out for compounds **34** and **42–44** using CB₂R-containing membranes (HTS020M2, Eurofins Discovery Services). To this end, membranes (5 μ g/well) were permeabilized by the addition of saponin (Sigma-Aldrich), then mixed with 0.3 nM [³⁵S]-GTP γ S (PerkinElmer) and 10 μ M GDP (Sigma-Aldrich) in 20 mM HEPES (Sigma-Aldrich) buffer containing 100 mM NaCl (Merck) and 10 mM MgCl₂ (Merck), at pH 7.4. Increasing concentrations of compounds **34** and **42–44** (from 10⁻¹¹ to 10⁻⁵ M) were added in a final volume of 100 μ L and incubated for 30 min at 30 °C. The nonspecific signal was measured with 10 μ M GTP γ S (Sigma-Aldrich). All 96-well plates and the tubes necessary for the experiment were previously silanized with Sigmacote (Sigma-Aldrich). The reaction was terminated by rapid vacuum filtration with a filter mate Harvester apparatus (PerkinElmer) through Filtermat A GF/C filters. The filters were washed nine times with ice-cold filtration buffer (10 mM sodium phosphate, pH 7.4), and bound radioactivity was measured with a 1450 LSC & Luminescence counter Wallac MicroBeta TriLux (PerkinElmer). [³⁵S]-GTP γ S binding data were analyzed to determine the EC₅₀ and E_{max} values by using an iterative curve-fitting procedure with GraphPad Prism, version 5.02 (GraphPad Software Inc.). EC₅₀ and E_{max} values are expressed as the mean \pm SEM of at least three experiments performed in triplicate for each point.

Molecular Modeling

Amino Acid Numbering—The numbering scheme for Class A GPCRs suggested by Ballesteros and Weinstein⁵⁷ was employed here. In this numbering system, the label 0.50 is assigned to the most highly conserved Class A residue in each transmembrane helix (TMH). This number is preceded by the TMH number and followed in parentheses by the sequence number. All other residues in a TMH are numbered relative to this residue.

Conformational Analysis of the Compounds—Global minimum energy conformations of **5**, **7b**, **18**, and **42** were determined with Spartan'08 (Wave function, Inc., Irvine CA) as follows: the structure of each molecule was built from the fragment library available in the program. Then, ab initio energy minimizations of each structure at the Hartree-Fock 6-31G* level were performed. A conformational search was next implemented using Molecular Mechanics (Monte Carlo method) followed by a minimization of the energy of each conformer calculated at the Hartree-Fock 6-31G* level. For this search, selected bonds were allowed to rotate: C–O bond in the phenolic ring, the first two C–C bonds of the dimethylheptyl chain, and the N–C bond in the ethyl substituent of the pyrazole. Representative conformers according to their geometry were selected for ab initio energy minimization (HF 6-31G*). The global minimum energy conformer of each compound was used as input for receptor docking studies.

Electrostatic Potential Map Calculation—The electrostatic potential density surface was calculated using Spartan'08 (Wave function, Inc., Irvine CA). The electrostatic potential energy was calculated using the Hartree-Fock method at the 6-31G* level of theory and was mapped on the 0.002 isodensity surface of each molecule. The surface was color-coded according to the potential, with electron rich regions colored red and electron poor regions colored blue.

CB₁R* and CB₂R* Models—The models used for these docking studies were developed by P. Reggio and co-workers.^{46,47} These models are based on the crystal structure of the class A GPCR, rhodopsin.⁵⁸ Complete details on the generation of the activated state models were published and properly described by them in the literature.^{43,46,59,60}

Docking Studies—Minimum energy conformers of each ligand were selected for the initial docking. Binding site anchoring interactions within the receptor for each ligand were based on earlier published docking studies for HU210⁴³ and for AM-841.^{44,45}

Initial steric clashes were removed manually with interactive graphics. The energy of the ligand-CBR* TMH bundle complex was minimized using the OPLS2005 force field in Macromodel (version 9.1, Schrödinger, LLC, New York, NY). An 8.0-Å extended nonbonded cutoff (updated every 10 steps), a 20.0-Å electrostatic cutoff, and a 4.0-Å hydrogen bond cutoff were used in each stage of the calculation. All residues except D2.50(163), K3.28(192), and D6.58(366) (CB₁R model), and D2.50(79), K3.28 (109), and D275 (CB₂R model), were neutralized during the minimization. C alpha atom restraints (100 kcal/mol) for all C alpha atoms were applied, and the full bundle was energy minimized until an energy gradient of 0.1 kcal/mol was reached. The C alpha atom restraints were then reduced in steps to 50 kcal/mol, and 0 kcal/mol (no restraints) until an energy gradient of 0.1 kcal/mol was achieved at each step. To allow the loops to adjust in their proper environment, atoms of the TMH regions were frozen, and the bundle was reminimized in water solvent to 0.1 kcal/mol gradient with loop residues fully charged.

Energy Expense Assessments for Docked Ligands—To calculate the energy difference between the global minimum energy conformer of each compound and its final conformation after energy minimization of the ligand–receptor complex, rotatable bonds in

the global minimum energy conformation were driven to their corresponding value in the final docked conformation, and the single point energy of the resultant structure was calculated at the HF 6-31G* level using Jaguar (version 9.1, Schrodinger, LLC, New York, NY).

Assessment of Pairwise Interaction Energies—After defining the atoms of each ligand as one group (group 1) and the atoms corresponding to a residue that lines the binding site in the final ligand-CB R* complex as another group (group 2), Macromodel (version 9.1, Schrödinger, LLC, New York, NY) was used to output the pairwise interaction energy (Coulombic and van der Waals) for a given pair of atoms. The pairs corresponding to group 1 (ligand) and group 2 (residue of interest) were then summed to yield the interaction energy between the ligand and that residue. Total interaction energy for each ligand with the cannabinoid receptor was calculated by summing the pairwise interaction energies for all residues in the binding site of that ligand and adding to this sum, the conformational energy expense for the ligand.

Animals and Theiler's Virus Infection

All experiments were performed in strict accordance with EU and governmental regulations (Decret 53/2013 BOE no. 34 and Comunidad de Madrid: ES 280790000184). The Ethics Committee on Animal Experimentation of the Instituto Cajal, CSIC approved all procedures described in this study (protocol number: 2013/03 CEEA-IC). Twelve-week-old female SJL/J mice (Harlan; Barcelona, Spain) were maintained at Cajal Institute (CSIC; Madrid, Spain) in an in-house colony under controlled conditions, on a 12 h light/dark cycle, temperature 20 °C (± 2 °C) and 40–50% relative humidity, with ad libitum access to food and water. Mice were intracerebrally inoculated in the right hemisphere with 2×10^6 plaque forming units (pfu) of the Daniel (DA) strain of Theiler's murine encephalomyelitis virus (TMEV), diluted in 30 μL of DMEM supplemented with 10% of fetal calf serum, as previously described.⁶¹ Sham mice received 30 μL of vehicle. Animals were injected intraperitoneally, for 7 consecutive days, with vehicle (10% DMSO in phosphate-buffered saline, PBS) or **43** (5 mg/kg).

Immunohistochemistry—Mice were anesthetized by intraperitoneal injection of pentobarbital (50 mg/kg body weight) and perfused transcardially with PBS. The brain of each animal was fixed in 4% paraformaldehyde (PFA) diluted in 0.1 M phosphate buffer (PB), cryoprotected in a 30% solution of sucrose in 0.1 M PB, and frozen at -80 °C until used. For immunofluorescence studies, the sections were rinsed three times for 10 min with 0.1 M PB, blocked as above, and then incubated overnight with the primary antibody against Iba1 (ionized calcium binding adaptor molecule 1, 1:1,000; Wako Chemical Pure Industry, Osaka, Japan). After washing three times for 10 min with 0.1 M PB, the sections were incubated for 1 h with an Alexa Fluor-conjugated secondary antibody (1:1,000; Molecular Probes Inc., Eugene, OR, USA). The sections were mounted with mowiol. Six brain sections per animal from at least 5 animals per group were analyzed. Quantification of staining was performed using the ImageJ software (NIH; Bethesda, MD, USA).

Statistical Analysis—The SPSS 22 software (IBM Corporation; USA) was used for the statistical analysis, applying the nonparametric Kruskal–Wallis test. All of the data are presented as the mean \pm standard error of mean (SEM). A value of $p < 0.05$ was considered statistically significant.

Supplementary Material

Refer to Web version on PubMed Central for supplementary material.

ACKNOWLEDGMENTS

Financial support was provided by Spanish Grants from the Spanish Ministry MINECO SAF2012-40075-C02-02, SAF2012-039875-C02-01, and SAF2015-68580-C2, by CAM S2010/BMD-2308, and by NIH Grants RO1 DA003934 and KO5 DA021358. C.G. and F.J.C.-S. thank REEM (Red Española de Esclerosis Múltiple; RD12/0032/0008) for its support. P.M. is a recipient of a fellowship JAE-Pre-2010-01119 from Junta para la Ampliación de Estudios cofinanced by FSE.

ABBREVIATIONS USED

CB	cannabinoid
ECS	endocannabinoid system
Fk	forskolin
MW	microwave
THC	tetrahydrocannabinol

TMEV-IDD Theiler's murine encephalomyelitis virus-induced demyelinating disease

REFERENCES

- (1). Matsuda LA, Lolait SJ, Brownstein MJ, Young AC, Bonner TI. Structure of a Cannabinoid Receptor and Functional Expression of the Cloned cDNA. *Nature*. 1990; 346(6284):561–564. [PubMed: 2165569]
- (2). Munro S, Thomas KL, Abu-Shaar M. Molecular Characterization of a Peripheral Receptor for Cannabinoids. *Nature*. 1993; 365(6441):61–65. [PubMed: 7689702]
- (3). Mechoulam R, Hanuš LO, Pertwee R, Howlett AC. Early Phytocannabinoid Chemistry to Endocannabinoids and Beyond. *Nat. Rev. Neurosci*. 2014; 15(11):757–764. [PubMed: 25315390]
- (4). Pacher P, Kunos G. Modulating the Endocannabinoid System in Human Health and Disease—Successes and Failures. *FEBS J*. 2013; 280(9):1918–1943. [PubMed: 23551849]
- (5). Alexander SPH. Therapeutic Potential of Cannabis-Related Drugs. *Prog. Neuro-Psychopharmacol. Biol. Psychiatry*. 2016; 64:157–166.
- (6). Fernández-Ruiz, J., Hernández, M., García-Movellán, Y. Cannabinoids and the Brain: New Hopes for New Therapies. In: Di Marzo, V., editor. *Cannabinoids*. John Wiley & Sons, Ltd.; Chichester, U.K.: 2014. p. 175-218.
- (7). Pertwee RG. Emerging Strategies for Exploiting Cannabinoid Receptor Agonists as Medicines. *Br. J. Pharmacol*. 2009; 156(3):397–411. [PubMed: 19226257]
- (8). Sharkey KA, Darmani NA, Parker LA. Regulation of Nausea and Vomiting by Cannabinoids and the Endocannabinoid System. *Eur. J. Pharmacol*. 2014; 722:134–146. [PubMed: 24184696]
- (9). Abrams DI, Guzman M. Cannabis in Cancer Care. *Clin. Pharmacol. Ther*. 2015; 97(6):575–586. [PubMed: 25777363]

- (10). Scherma, M., Satta, V., Fratta, W., Fadda, P. Cannabinoids in Neurologic and Mental Disease. Elsevier; Oxford, U.K.: 2015. The Endocannabinoid System: Anorexia Nervosa and Binge Eating Disorder; p. 389-413.
- (11). Meuth SG, Vila C, Dechant KL. Effect of Sativex on Spasticity-Associated Symptoms in Patients with Multiple Sclerosis. *Expert Rev. Neurother.* 2015; 15(8):909–918. [PubMed: 26166264]
- (12). Scheen, a J. CB1 Receptor Blockade and Its Impact on Cardiometabolic Risk Factors: Overview of the RIO Programme with Rimonabant. *J. Neuroendocrinol.* 2008; 20(Suppl 1):139–146.
- (13). Picone RP, Kendall D. Minireview: From the Bench, Toward the Clinic: Therapeutic Opportunities for Cannabinoid Receptor Modulation. *Mol. Endocrinol.* 2015; 29(6):801–813. [PubMed: 25866875]
- (14). Gong J-P, Onaivi ES, Ishiguro H, Liu Q-R, Tagliaferro PA, Brusco A, Uhl GR. Cannabinoid CB2 Receptors: Immunohistochemical Localization in Rat Brain. *Brain Res.* 2006; 1071(1):10–23. [PubMed: 16472786]
- (15). Van Sickle MD, Duncan M, Kingsley PJ, Mouihate A, Urbani P, Mackie K, Stella N, Makriyannis A, Piomelli D, Davison JS, Marnett LJ, Di Marzo V, Pittman QJ, Patel KD, Sharkey KA. Identification and Functional Characterization of Brainstem Cannabinoid CB2 Receptors. *Science.* 2005; 310(5746):329–332. [PubMed: 16224028]
- (16). Ashton JC, Friberg D, Darlington CL, Smith PF. Expression of the Cannabinoid CB2 Receptor in the Rat Cerebellum: An Immunohistochemical Study. *Neurosci. Lett.* 2006; 396(2):113–116. [PubMed: 16356641]
- (17). Sierra S, Luquin N, Rico AJ, Gómez-Bautista V, Roda E, Dopeso-Reyes IG, Vázquez A, Martínez-Pinilla E, Labandeira-García JL, Franco R, Lanciego JL. Detection of Cannabinoid Receptors CB1 and CB2 within Basal Ganglia Output Neurons in Macaques: Changes Following Experimental Parkinsonism. *Brain Struct. Funct.* 2015; 220(5):2721–2738. [PubMed: 24972960]
- (18). Lanciego JL, Barroso-Chinea P, Rico AJ, Conte-Perales L, Callén L, Roda E, Gómez-Bautista V, López IP, Lluís C, Labandeira-García JL, Franco R. Expression of the mRNA Coding the Cannabinoid Receptor 2 in the Pallidal Complex of Macaca Fascicularis. *J. Psychopharmacol.* 2011; 25(1):97–104. [PubMed: 20488834]
- (19). Han S, Thatte J, Buzard DJ, Jones RM. Therapeutic Utility of Cannabinoid Receptor Type 2 (CB2) Selective Agonists. *J. Med. Chem.* 2013; 56(21):8224–8256. [PubMed: 23865723]
- (20). Boychuk DG, Goddard G, Mauro G, Orellana MF. The Effectiveness of Cannabinoids in the Management of Chronic Nonmalignant Neuropathic Pain: A Systematic Review. *J. Oral Facial Pain Headache.* 2015; 29(1):7–14. [PubMed: 25635955]
- (21). Rahman W, Dickenson AH. Emerging Targets and Therapeutic Approaches for the Treatment of Osteoarthritis Pain. *Curr. Opin. Support. Palliat. Care.* 2015; 9(2):124–130. [PubMed: 25730180]
- (22). Ofek O, Karsak M, Leclerc N, Fogel M, Frenkel B, Wright K, Tam J, Attar-namdar M, Kram V, Shohami E, Mechoulam R, Zimmer A, Bab I. Peripheral Cannabinoid Receptor, CB2, Regulates Bone Mass. *Proc. Natl. Acad. Sci. U. S. A.* 2006; 103(3):696–701. [PubMed: 16407142]
- (23). Dhopeshwarkar A, Mackie K. CB2 Cannabinoid Receptors as a Therapeutic Target - What Does the Future Hold? *Mol. Pharmacol.* 2014; 86(4):430–437.
- (24). Gowran A, Noonan J, Campbell V. a. The Multiplicity of Action of Cannabinoids: Implications for Treating Neurodegeneration. *CNS Neurosci. Ther.* 2011; 17(6):637–644. [PubMed: 20875047]
- (25). Gómez-Gálvez Y, Palomo-Garo C, Fernández-Ruiz J, García C. Potential of the Cannabinoid CB2 Receptor as a Pharmacological Target against Inflammation in Parkinson's Disease. *Prog. NeuroPsychopharmacol. Biol. Psychiatry.* 2016; 64:200–208. [PubMed: 25863279]
- (26). Feliú A, Moreno-Martet M, Mecha M, Carrillo-Salinas FJ, de Lago E, Fernández-Ruiz J, Guaza C. A Sativex-like Combination of Phytocannabinoids as a Disease-Modifying Therapy in a Viral Model of Multiple Sclerosis. *Br. J. Pharmacol.* 2015; 172:3579–3595. [PubMed: 25857324]
- (27). Rom S, Persidsky Y. Cannabinoid Receptor 2: Potential Role in Immunomodulation and Neuroinflammation. *J. Neuroimmune Pharmacol.* 2013; 8(3):608–620. [PubMed: 23471521]
- (28). Han S, Thatte J, Buzard DJ, Jones RM. Therapeutic Utility of Cannabinoid Receptor Type 2 (CB2) Selective Agonists. *J. Med. Chem.* 2013; 56(21):8224–8256. [PubMed: 23865723]

- (29). Fernández-Ruiz J. The Endocannabinoid System as a Target for the Treatment of Motor Dysfunction. *Br. J. Pharmacol.* 2009; 156(7):1029–1040. [PubMed: 19220290]
- (30). Velayudhan L, Van Diepen E, Marudkar M, Hands O, Suribhatla S, Prettyman R, Murray J, Baillon S, Bhattacharyya S. Therapeutic Potential of Cannabinoids in Neurodegenerative Disorders: A Selective Review. *Curr. Pharm. Des.* 2014; 20:2218–2230. [PubMed: 23829360]
- (31). Docagne F, Mestre L, Loría F, Hernangómez M, Correa F, Guaza C. Therapeutic Potential of CB2 Targeting in Multiple Sclerosis. *Expert Opin. Ther. Targets.* 2008; 12(2):185–195. [PubMed: 18208367]
- (32). Pryce G, Baker D. Potential Control of Multiple Sclerosis by Cannabis and the Endocannabinoid System. *CNS Neurol. Disord.: Drug Targets.* 2012; 11:624–641. [PubMed: 22583441]
- (33). Han S, Chen JJ, Chen JZ. Latest Progress in the Identification of Novel Synthetic Ligands for the Cannabinoid CB2 Receptor. *Mini-Rev. Med. Chem.* 2014; 14(5):426–443. [PubMed: 24766386]
- (34). Cumella J, Hernández-Folgado L, Girón R, Sánchez E, Morales P, Hurst DP, Gómez-Cañas M, Gómez-Ruiz M, Pinto DCGA, Goya P, Reggio PH, Martin MI, Fernández-Ruiz J, Silva AMS, Jagerovic N. Chromenopyrazoles: Non-Psychoactive and Selective CB1 Cannabinoid Agonists with Peripheral Antinociceptive Properties. *ChemMedChem.* 2012; 7(3):452–463. [PubMed: 22302767]
- (35). Mecha M, Carrillo-Salinas FJ, Mestre L, Feliú A, Guaza C. Viral Models of Multiple Sclerosis: Neurodegeneration and Demyelination in Mice Infected with Theiler's Virus. *Prog. Neurobiol.* 2013; 101–102(1):46–64.
- (36). Gómez-Cañas M, Morales P, García-Toscano L, Gómez-Cañas; Maria Navarrete C, Muñoz E, Jagerovic N, Fernández-Ruiz J, García-Arencibia M, Pazos R. Biological Characterization of PM226, a Chromenoisoxazole, As a Selective CB2 Receptor Agonist with Neuroprotective Profile. *Pharmacol. Res.* 2016; 110:205–215. [PubMed: 27013280]
- (37). Hanus L, Breuer A, Tchilibon S, Shiloah S, Goldenberg D, Horowitz M, Pertwee RG, Ross RA, Mechoulam R, Fride E. HU-308: A Specific Agonist for CB2, a Peripheral Cannabinoid Receptor. *Proc. Natl. Acad. Sci. U. S. A.* 1999; 96(25):14228–14233. [PubMed: 10588688]
- (38). Huffman JW, Liddle J, Yu S, Aung MM, Abood ME, Wiley JL, Martin BR. 3-(1',1'-Dimethylbutyl)-1-Deoxy-8-THC and Related Compounds: Synthesis of Selective Ligands for the CB2 Receptor. *Bioorg. Med. Chem.* 1999; 7(12):2905–2914. [PubMed: 10658595]
- (39). Melvin LS, Johnson MR, Harbert CA, Milne GM, Weissman A. A Cannabinoid Derived Prototypical Analgesic. *J. Med. Chem.* 1984; 27(1):67–71. [PubMed: 6690685]
- (40). Huffman JW, Bushell SM, Miller J. R. a, Wiley L, Martin BR. New Selective Ligands for the CB2 Receptor. *Bioorg. Med. Chem.* 2002; 10:4119–4129. [PubMed: 12413866]
- (41). Hernandez-Folgado L, Cumella JM, Morales P, Alkorta I, Elguero J, Jagerovic N. Tautomerism of Hydroxychromenopyrazoles. *J. Mol. Struct.* 2012; 1015:162–165.
- (42). Reggio PH. Cannabinoid Receptors and Their Ligands: Ligand-Ligand and Ligand-Receptor Modeling Approaches. *Handb. Exp. Pharmacol.* 2005; 168:247–281.
- (43). Kapur A, Hurst DP, Fleischer D, Whitnell R, Thakur GA, Makriyannis A, Reggio PH, Abood ME. Mutation Studies of SER7.39 and Ser2.60 in the Human CB1 Cannabinoid Receptor: Evidence for a Serine-Induced Bend in CB1 Transmembrane Helix 7. *Mol. Pharmacol.* 2007; 71(6):1512–1524. [PubMed: 17384224]
- (44). Nebane NM, Hurst DP, Carrasquer C, Qiao Z, Reggio PH, Song ZH. Residues Accessible in the Binding-Site Crevice of Transmembrane Helix 6 of the CB2 Cannabinoid Receptor. *Biochemistry.* 2008; 47(52):13811–13821. [PubMed: 19053233]
- (45). Pei Y, Mercier RW, Anday JK, Thakur GAM, Zvonok A, Hurst D, Reggio PH, Janero DR, Makriyannis A. Ligand-Binding Architecture of Human CB2 Cannabinoid Receptor: Evidence for Receptor Subtype-Specific Binding Motif and Modeling GPCR Activation. *Chem. Biol.* 2008; 15(11):1207–1219. [PubMed: 19022181]
- (46). Hurst DP, Grossfield A, Lynch DL, Feller S, Romo TD, Gawrisch K, Pitman MC, Reggio PH. A Lipid Pathway for Ligand Binding Is Necessary for a Cannabinoid G Protein-Coupled Receptor. *J. Biol. Chem.* 2010; 285(23):17954–17964. [PubMed: 20220143]
- (47). Zhang R, Hurst DP, Barnett-Norris J, Reggio PH, Song Z-H. Cysteine 2.59(89) in the Second Transmembrane Domain of Human CB2 Receptor Is Accessible within the Ligand Binding

- Crevice: Evidence for Possible CB2 Deviation from a Rhodopsin Template. *Mol. Pharmacol.* 2005; 68(1):69–83. [PubMed: 15840841]
- (48). Picone RP, Khanolkar AD, Xu W, Ayotte LA, Thakur GA, Hurst DP, Abood ME, Reggio PH, Fournier DJ, Makriyannis A. (–)-7'-Isothiocyanato-11-Hydroxy-1', 1'-Dimethylheptylhexahydrocannabinol (AM841), a High-Affinity Electrophilic Ligand, Interacts Covalently with a Cysteine in Helix Six and Activates the CB1 Cannabinoid Receptor. *Mol. Pharmacol.* 2005; 68(6):1623–1635. [PubMed: 16157695]
- (49). Hurst D, Lynch D, Barnett-Norris J, Hyatt S, Seltzman H, Zhong M, Song Z, Nie J, Lewis D, Reggio P. N-(Piperidin-1-Yl)-5-(4-Chlorophenyl)-1-(2,4-Dichlorophenyl)-4-Methyl-1H-Pyrazole-3-Carboxamide (SR141716A) Interaction with LYS 3.28(192) Is Crucial for Its Inverse Agonism at the Cannabinoid CB1 Receptor. *Mol. Pharmacol.* 2002; 62(6):1274–1287. [PubMed: 12435794]
- (50). Rinaldi-Carmona M, Barth F, Millan J, Derocq JM, Casellas P, Congy C, Oustric D, Sarran M, Bouaboula M, Calandra B, Portier M, Shire D, Breliere JC, Le Fur GL. SR 144528, the First Potent and Selective Antagonist of the CB2 Cannabinoid Receptor. *J. Pharmacol. Exp. Ther.* 1998; 284(2):644–650. [PubMed: 9454810]
- (51). Compton DR, Gold LH, Ward SJ, Balster RL, Martin BR. Aminoalkylindole Analogs: Cannabimimetic Activity of a Class of Compounds Structurally Distinct from Delta 9-Tetrahydrocannabinol. *J. Pharmacol. Exp. Ther.* 1992; 263(3):1118–1126. [PubMed: 1335057]
- (52). Fernández-Ruiz J, Romero J, Velasco G, Tólon RM, Ramos J. a. Guzmán M. Cannabinoid CB2 Receptor: A New Target for Controlling Neural Cell Survival? *Trends Pharmacol. Sci.* 2007; 28(1):39–45. [PubMed: 17141334]
- (53). Miller, a M., Stella, N. CB2 Receptor-Mediated Migration of Immune Cells: It Can Go Either Way. *Br. J. Pharmacol.* 2008; 153(2):299–308. [PubMed: 17982478]
- (54). Palazuelos J, Davoust N, Julien B, Hatterer E, Aguado T, Mechoulam R, Benito C, Romero J, Silva A, Guzman M, Nataf S, Galve-Roperh I. The CB2 Cannabinoid Receptor Controls Myeloid Progenitor Trafficking. *J. Biol. Chem.* 2008; 283(19):13320–13329. [PubMed: 18334483]
- (55). Vela M, Molina-holgado E, Guaza C. Therapeutic Action of Cannabinoids in a Murine Model of Multiple Sclerosis. *J. Neurosci.* 2003; 23(7):2511–2516. [PubMed: 12684434]
- (56). Mestre L, Iñigo PM, Mecha M, Correa FG, Hernangómez-Herrero M, Loría F, Docagne F, Borrell J, Guaza C. Anandamide Inhibits Theiler's Virus Induced VCAM-1 in Brain Endothelial Cells and Reduces Leukocyte Transmigration in a Model of Blood Brain Barrier by Activation of CB1 Receptors. *J. Neuroinflammation.* 2011; 8(1):102. [PubMed: 21851608]
- (57). Ballesteros, JA., Weinstein, H. Integrated Methods for the Construction of Three-Dimensional Models and Computational Probing of Structure-Function Relations in G Protein-Coupled Receptors. In: Sealfon, SC., editor. *Methods in Neurosciences*. Vol. 25. Academic Press; San Diego, CA: 1995. p. 366-428.
- (58). Palczewski K, Kumasaka T, Hori T, Behnke CA, Motoshima H, Fox BA, Le Trong I, Teller DC, Okada T, Stenkamp RE, Yamamoto M, Miyano M. Crystal Structure of Rhodopsin: A G Protein-Coupled Receptor. *Science.* 2000; 289(5480):739–745. [PubMed: 10926528]
- (59). Mnpotra JS, Qiao Z, Cai J, Lynch DL, Grossfield A, Leioatts N, Hurst DP, Pitman MC, Song Z-H, Reggio PH. *J. Biol. Chem.* 2014; 289:20259.
- (60). Reggio PH. Computational Methods in Drug Design: Modeling G Protein-Coupled Receptor Monomers, Dimers, and Oligomers. *AAPS J.* 2006; 8(2):E322–E336. [PubMed: 16796383]
- (61). Lledó A, Borrell J, Guaza C. Dexamethasone regulation of interleukin-1-receptors in the hippocampus of Theiler's virus-infected mice: effects on virus-mediated demyelination. *Eur. J. Pharmacol.* 1999; 372(1):75–83. [PubMed: 10374717]

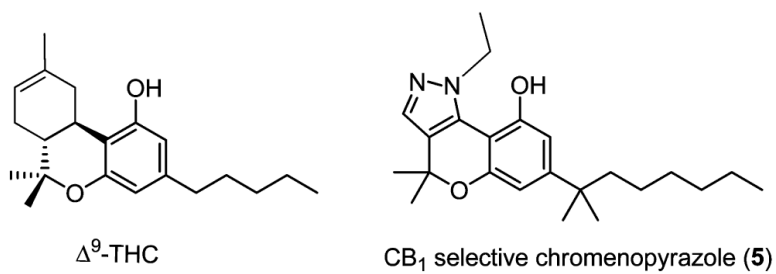


Figure 1. Structures of Δ^9 -tetrahydrocannabinoid (Δ^9 -THC) and the previously identified CB₁ fully selective chromenopyrazoles.³⁴

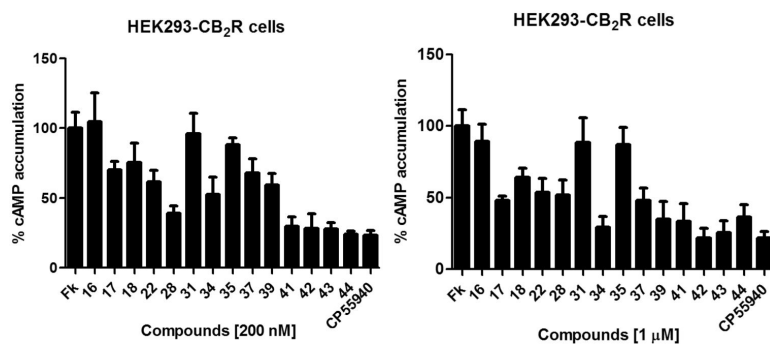


Figure 2. cAMP screening in HEK293-CB₂R cells. Results are expressed as percent of forskolin (Fk)-stimulated cAMP accumulation at a concentration of 200 nM and 1 μM of **16–18, 22, 28, 31, 34, 35, 37, 39, or 41–44**. All data result from at least three independent experiments, performed in triplicate.

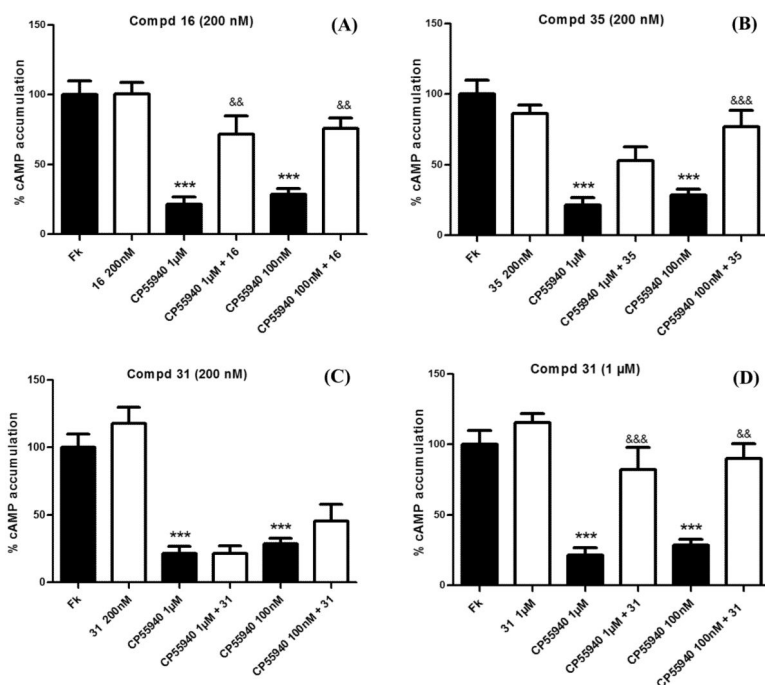


Figure 3. Effect of compounds **16**, **31**, and **35** on CP55,940-induced inhibition of cAMP accumulation in HEK293-CB2R cells. (A) **16** at 200 nM; (B) **34** at 200 nM; (C) **31** at 200 nM; (D) **31** at 1 μ M. All data result from at least three independent experiments, performed in triplicate. Data were assessed by one-way analysis of variance ($F(5,43) = 20.57$, $p < 0.0001$ for **16**; $F(5,42) = 17.92$, $p < 0.0001$ for **35**; $F(5,33) = 27.16$, $p < 0.0001$ for **31** (C); $F(5,33) = 22.03$, $p < 0.0001$ for **31** (D)); * $p < 0.05$, ** $p < 0.01$, *** $p < 0.005$ compounds alone versus control (Fk cAMP accumulation); and $p < 0.05$, $p < 0.01$, and $p < 0.005$ CB₂ agonist versus CB₂ agonist + **16**, **31**, or **35**.

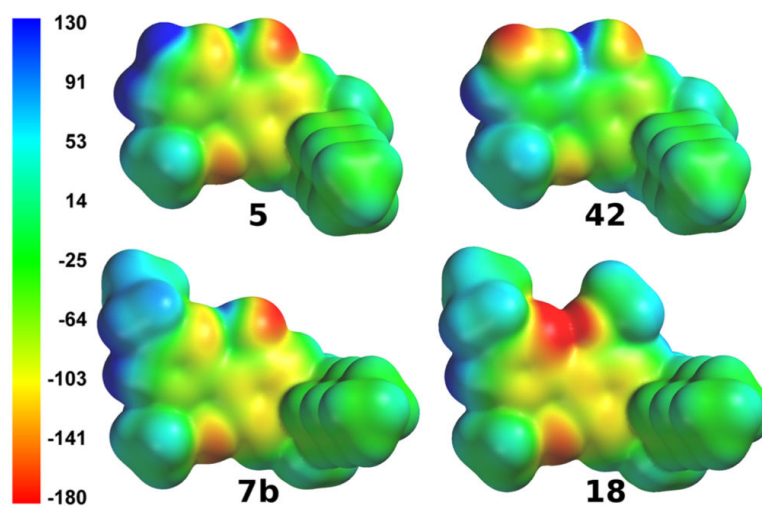


Figure 4. Molecular electrostatic potential maps of the minimum energy conformations of **5**, **7b**, **18**, and **42** are illustrated here. The electrostatic potential scale (in kJ/mol) is provided as a color scale. This scale is from blue (most electropositive) to red (most electronegative).

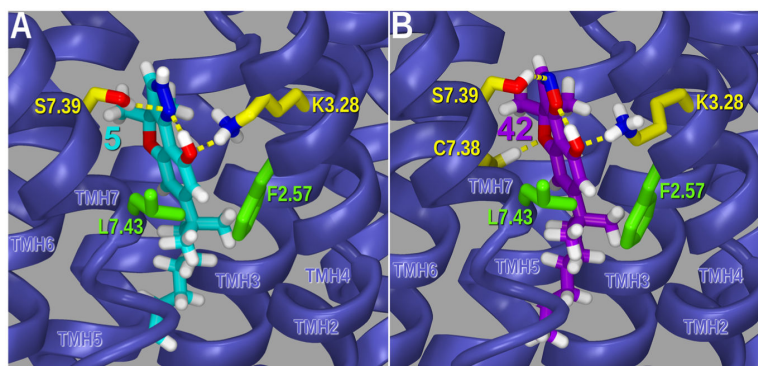


Figure 5. Binding site of 5 (panel A) and 42 (panel B) in the CB₁R* model. Side view of ligand/receptor complexes as if looking through TMH1 (not displayed). Hydrophilic interacting residues are represented with yellow carbons. Hydrogen bonds are shown with yellow dashed lines. Select hydrophobic interacting residues, F2.57 and L7.43, are displayed with green carbons.

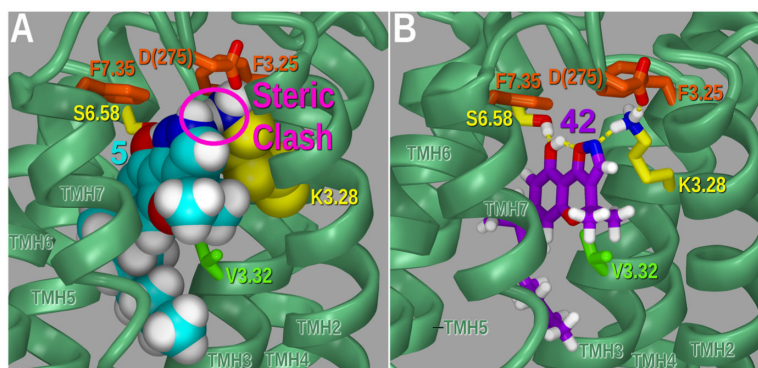


Figure 6. Binding site of 42 (panel B, in purple) in the CB₂R* model. Side view of the ligand/receptor complex as if looking through TMH1 (not displayed). Hydrophilic interacting residues are represented with yellow carbons. Hydrogen bonds are shown with yellow dash lines. A selected hydrophobic interacting residue, V3.32, is displayed with green carbons. Structure of 5 (panel A, in cyan) was superimposed on the 42-CB₂R* complex. The magenta circle indicates van der Waals steric overlap of 5 with K3.28, which forms a salt bridge with D(275) in the CB₂R* binding site.

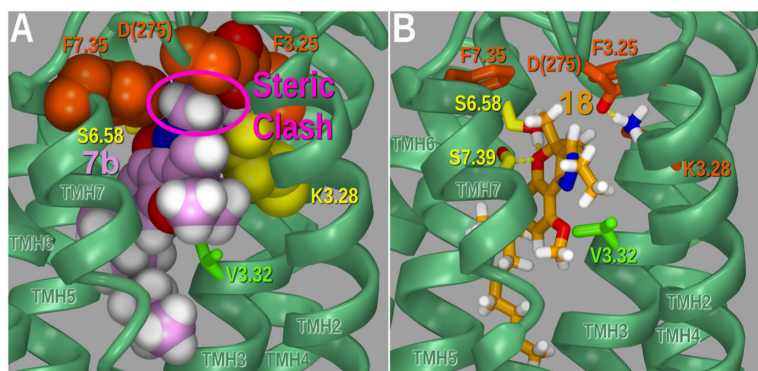


Figure 7. Binding site of **18** (panel B, in orange) in the CB₂R* model. Side view of the ligand/receptor complex as if looking through TMH1 (not displayed). Hydrophilic interacting residues are represented with yellow carbons. Hydrogen bonds are shown with yellow dash lines. A selected hydrophobic interacting residue, V3.32, is displayed with green carbons. Structure of **7b** (panel A, in pink) was superimposed on the **42**-CB₂R* complex. The magenta circle indicates van der Waals steric overlap with K3.28, D(275), and F7.35. The residues K3.28 and D(275) form a salt bridge within the CB₂R* binding site.

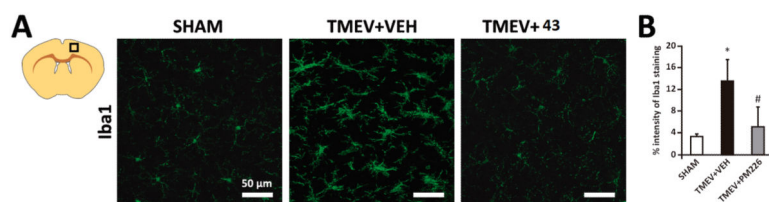
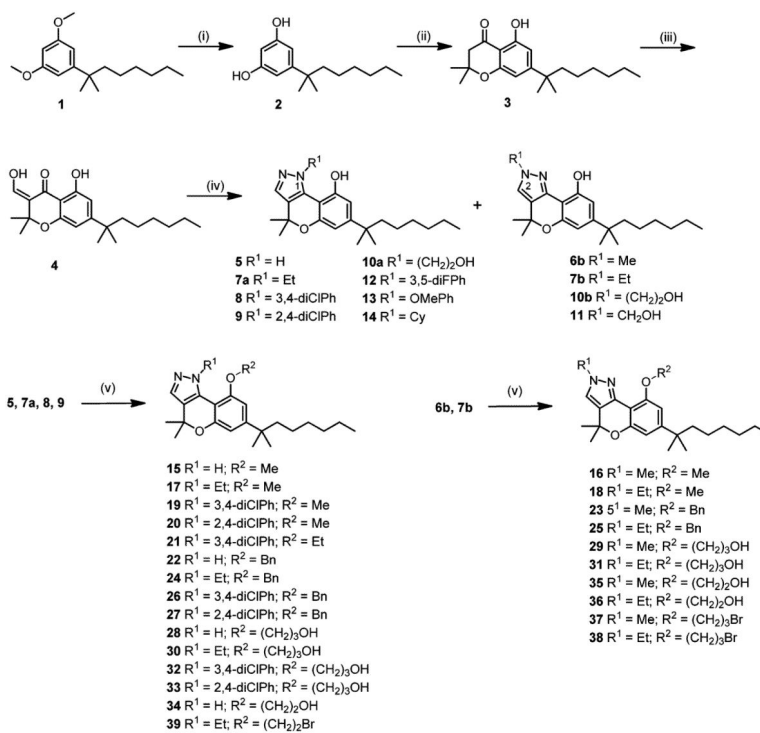
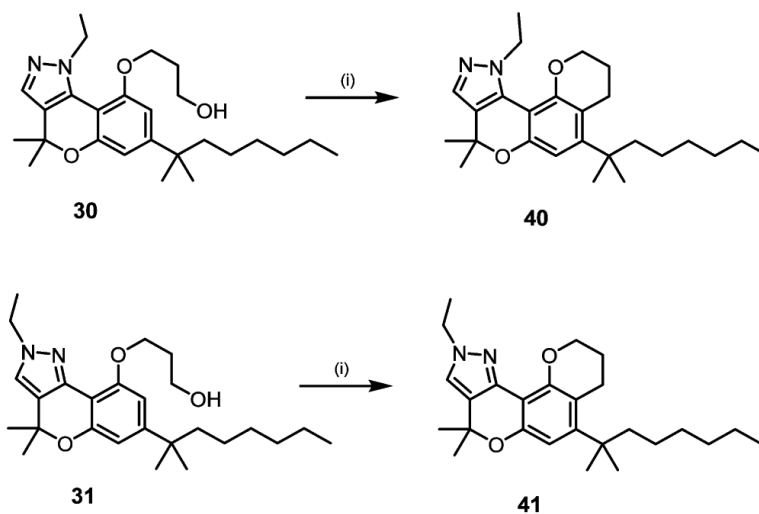


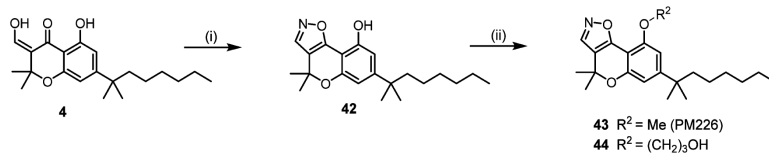
Figure 8. Compound 43 significantly reduces microglial activation on TMEV-infected mice. (A) Brain sections were stained with an anti-Iba1 Ab for microglia labeling and analyzed by confocal microscopy. Representative images are shown. Fluorescence intensity was measured with ImageJ software and plotted to show quantification of the analyzed images (B), mean \pm SEM * $p < 0.05$ vs Sham, # $p < 0.05$ vs TMEV+veh, in a nonparametric Kruskal–Wallis test. Scale bar: 50 μ m.



Scheme 1.
 Synthesis of Chromenopyrazoles 5–39^a

^aReagents and conditions: (i) BBr₃, CH₂Cl₂, overnight, from 0 °C to rt, 92%; (ii) 3,3-dimethylacrylic acid, methanesulfonic acid, P₂O₅, 8 h, 70 °C, 81%; (iii) (a) NaH, THF, MW, 25 min, 45 °C; (b) ethyl formate, MW, 25 min, 45 °C, 76%; (iv) corresponding hydrazine, EtOH, 1–4 h, 40 °C, 36–50%; (v) (a) NaH, THF, 10 min, (b) 1-bromo or iodoalkane, 8–72 h, reflux, 36–50%.

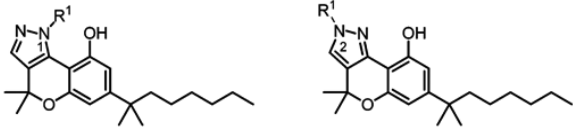
**Scheme 2.**Synthesis of Pyrano-chromenopyrazoles 40 and 41^a^aReagents and conditions: (i) P₂O₅, toluene, 3 h, reflux, 36–66%.

**Scheme 3.**Synthesis of Chromenoisoxazoles 42–44^a

^aReaction conditions: (i) hydroxylamine hydrochloride, acetic acid, 15 min, reflux, 91%; (ii) (a) NaH, THF, 10 min, 0 °C; (b) 1-bromo or iodoalkane, 8–72 h, reflux, 36–50%.

Table 1

Binding Affinity of Chromenopyrazoles 5–14 and Reference Cannabinoids for hCB₁ and hCB₂ Cannabinoid Receptors



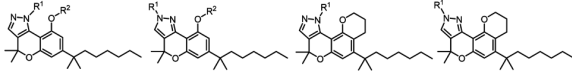
compd	R ¹	CB ₁	CB ₂	CB ₁	CB ₂
		K _i (nM) ^a	K _i (nM) ^a	select ^b	select ^c
5 ³⁴	H	28.5 ± 23.7	>40000	>1400	
6b ³⁴	N2-Me	14.2 ± 2.9	>40000	>2500	
7a ³⁴	N1-Et	4.5 ± 0.6	>40000	>8000	
7b ³⁴	N2-Et	18.6 ± 2.9	>40000	>2000	
8 ³⁴	N1-3,4-diClPh	514 ± 205	270		1.9
9 ³⁴	N1-2,4-diClPh	5.2 ± 4.3	>40000	>7500	
10a	N1-(CH ₂) ₂ OH	19.1 ± 8.9	366 ± 169	19.1	
10b	N2-(CH ₂) ₂ OH	54.4 ± 8.1	39.6 ± 7.1		1.4
11	N2-CH ₂ OH	218.1 ± 40.5	59.4 ± 31.2		3.7
12	N1-3,5-diFPh	>40000	>40000		
13	N1-3-OMePh	6440 ± 655	562.0 ± 13.2		11.5
14	N1-Cy	1140 ± 190	53.7 ± 11.8	-	21.5
SR141716		7.3 ± 0.9	>40000	>5400	
WIN55,212-2		45.6 ± 8.6	3.7 ± 0.2		12.3

^a K_i: affinity constants. Values were obtained from competition curves using [³H]CP55940 as radioligand for hCB₁ and hCB₂ cannabinoid receptors and are expressed as the mean ± SEM of at least three experiments.

^b K_i(CB₁)/K_i(CB₂) selectivity ratio.

^c K_i(CB₂)/K_i(CB₁) selectivity ratio.

Table 2

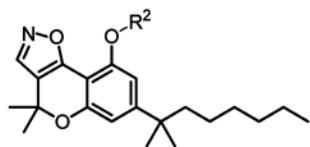
Binding Affinity of Chromenopyrazoles 15–41 for hCB₁ and hCB₂ Cannabinoid Receptors


compd	R ¹	R ²	CB ₁	CB ₂	CB ₁	CB ₂
			K _i (nM) ^a	K _i (nM) ^a	select ^b	select ^c
15	H	Me	272 ± 75	87.1 ± 10.6		3.1
16	N2-Me	Me	4159 ± 542	66.4 ± 13.29		62.6
17	N1-Et	Me	5040 ± 670	159.5 ± 31.2		31.6
18	N2-Et	Me	2930 ± 470	92.6 ± 17.1		31.8
19	N1-3,4-diClPh	Me	2324 ± 327	2256 ± 499		
20	N1-2,4-diClPh	Me	1693 ± 239	1493 ± 272		
21	N1-3,4-diClPh	Et	>40000	3545 ± 89		>11.3
22	H	Bn	22.4 ± 4.1	93.3 ± 29.5	4.2	
23	N2-Me	Bn	702.4 ± 98.6	208.8 ± 39.5		3.3
24	N1-Et	Bn	613.7 ± 206.9	295.9 ± 53.6		2.0
25	N2-Et	Bn	671.3 ± 166.1	212.2 ± 49.4		3.1
26	N1-3,4-diClPh	Bn	>40000	3740 ± 297		>10.7
27	N1-2,4-diClPh	Bn	>40000	>40000		
28	H	(CH ₂) ₃ OH	450.4 ± 9.9	26.0 ± 7.1		17.3
29	N2-Me	(CH ₂) ₃ OH	>40000	364.0 ± 68.9		>109.9
30	N1-Et	(CH ₂) ₃ OH	1613 ± 284	440 ± 145		3.6
31	N2-Et	(CH ₂) ₃ OH	>40000	97.4 ± 9.9		>410.7
32	N1-2,4-diClPh	(CH ₂) ₃ OH	>40000	>40000		
33	N1-3,4-diClPh	(CH ₂) ₃ OH	>40000	>40000		
34	H	(CH ₂) ₂ OH	64.8 ± 18.0	3.6 ± 0.7		18
35	N2-Me	(CH ₂) ₂ OH	1086 ± 198	39.8 ± 24.9		27.2
36	N2-Et	(CH ₂) ₂ OH	6512 ± 714	210.6 ± 93.2		31.0
37	N2-Me	(CH ₂) ₃ Br	1482 ± 221	77.3 ± 0.87		19.1
38	N2-Et	(CH ₂) ₃ Br	657 ± 159	87.1 ± 14.2		7.5
39	N1-Et	(CH ₂) ₂ Br	1331 ± 320	78.7 ± 11.3		16.9
40	N1-Et		>10000	563.8 ± 13.1		>17.7
41	N2-Et		>40000	121.6 ± 43.5		>330.5

^a K_i: affinity constants. Values were determined from competition curves using [³H]CP55940 as radioligand for hCB₁ and hCB₂ cannabinoid receptors and are expressed as the mean ± SEM of at least three experiments.

^b K_i(CB₁)/K_i(CB₂) selectivity ratio.

^c K_i(CB₂)/K_i(CB₁) selectivity ratio.

Table 3Binding Affinity of Chromenoisoxazoles 42-44 for hCB₁ and hCB₂ Cannabinoid Receptors

compd	R ²	CB ₁	CB ₂	CB ₁	CB ₂
		K _i (nM) ^a	K _i (nM) ^a	select ^b	select ^c
42	H	15.4 ± 12.2	5.3 ± 0.8		2.9
43	Me	>40000	12.8 ± 2.4		>3100
44	(CH ₂) ₃ OH	332.6 ± 143.9	65.5 ± 21.8		5.1

^aK_i: affinity constants. Values were obtained from competition curves using [³H]CP55940 as radioligand for hCB₁ and hCB₂ cannabinoid receptors and are expressed as the mean ± SEM of at least three experiments.

^bK_i(CB₁)/K_i(CB₂) selectivity ratio.

^cK_i(CB₂)/K_i(CB₁) selectivity ratio.

Table 4

Functional Potencies of 34 and 41–44 and Reference Cannabinoids at the CB₂ Receptor Determined by Measuring the Decrease in Forskolin-Stimulated cAMP Levels in HEK293-CB2R Cells or by [³⁵S]-GTPγS Binding to the hCB₂ Receptor

compd	cAMP assay (CB ₂ R)		[³⁵ S]-GTPγS assays (CB ₂ R)	
	IC ₅₀ ^a (nM)	E _{max} ^b (%)	IC ₅₀ ^c (nM)	E _{max} ^d (%)
34	21.6 ± 1.5	95 ± 6	95.1 ± 7.2	110 ± 17
41	25.5 ± 2.0	98 ± 11	n.d.	n.d.
42	134.0 ± 2.3	98 ± 9	50.2 ± 24.9	114 ± 37
43	4.2 ± 1.5	101 ± 10	38.6 ± 6.7	98 ± 8
44	14.0 ± 1.9	91 ± 10	539.6 ± 208.1	96 ± 15
CP55,940	8.3 ± 1.5	100 ± 9	n.d.	n.d.
JWH133	81.8 ± 1.7	98 ± 11	n.d.	n.d.
HU308	n.d.	n.d.	64.5 ± 1.6	91 ± 7

^aIC₅₀ values were calculated using nonlinear regression analysis. Data are expressed as the mean ± SEM of at least three independent experiments, each one run in triplicate.

^bForskolin stimulated cAMP levels were normalized to 100%. E_{max} is the maximum inhibition of forskolin stimulated cAMP levels.

^cEC₅₀ values were calculated using nonlinear regression analysis. Data are expressed as the mean ± SEM of at least three independent experiments, each one run in triplicate.

^dE_{max}: maximal agonist effect, determined using nonlinear regression analysis.

Table 5

[³⁵S]-GTP γ S Binding of Compounds 10b, 22, and 42 and the Reference Cannabinoid WIN55,212-2 to hCB₁ Receptor

compd	[³⁵ S]-GTP γ S assays (CB ₁ R)	
	EC ₅₀ ^a (nM)	E _{max} ^b (%)
10b	298.8 ± 54.2	97 ± 52
22	191.0 ± 90.8	234 ± 79
42	15.8 ± 8.6	196 ± 111
WIN55,212	44 ± 30	153 ± 70

^aEC₅₀ values were calculated using nonlinear regression analysis. Data are expressed as the mean ± SEM of at least three independent experiments, each one run in triplicate.

^bE_{max}: maximal agonist effect, determined using nonlinear regression analysis.